

## **Part 5**

---

### **FUNDAMENTAL UNITY OF HEAT AND NON-HEAT FORMS-OF-ENERGY CONVERSION PROCESSES**

The development logic for a whole number of scientific disciplines dictates the necessity to supplement the classic theory of thermal engines with an analysis of interrelation between the thermodynamic efficiency and power of various-kind energy converters (thermal and nonthermal, cyclic and non-cyclic, direct and reverse). The kinetics of useful energy conversion processes is interesting to not only power engineering and power processing, for which these processes are fundamental. The thermodynamic investigation of biological systems and the processes of their self-organization studied by synergetics is either impossible without due consideration for the work supporting the nonequilibrium state of such systems and providing their vital activity. The application of thermodynamics to cosmological objects that develop, according to the modern considerations, omitting the equilibrium state would also be incomplete without taking into consideration the work as an ordered form of energy exchange.

In this context a necessity appears to generalize the methods of irreversible process kinetics analysis to the useful energy conversion processes and to create on this basis a single theory of energy conversion process rate and productivity, which would relate to the classic theory of thermal engines in the same manner as dynamics to statics.

## **Chapter 18**

### **SIMILARITY THEORY FOR ENERGY CONVERTING SYSTEMS**

Classic thermodynamics, having time excluded from its equations, did not consider the processes of energy and its carriers transfer. Therefore the issue regarding unity of energy transfer and conversion processes could not arise in its depths. N. Umov was the first (1873) who paid attention to that relation and stated the energy conservation law (2.3.6) for me-

chanical processes rather as a consequence of energy transfer across the system borders than as a result of energy disappearing in some points of space and appearing in others. It remained unanswered, however, what was the “transfer substrate” in that case – either the material energy carriers attributed to the extensive values  $\Theta_i$  category or the intensive values  $\psi_i$  as analogs of mechanical stresses. Thermokinetics gives an answer to this question. According to (2.3.10) the flux  $\mathbf{J}_{ui}$  of any  $i^{\text{th}}$  form of energy is expressed as the product of the intensive measure of motion – the generalized potential  $\psi_i$  – and the energy carrier flux  $\mathbf{J}_i$  that is defined, in its turn, as the product of the extensive measure of motion  $\Theta_i$  of this particular kind being transferred and the velocity  $\mathbf{v}_i$  of its transfer in space. This flux density  $\mathbf{j}_i$  is accordingly expressed as the product of the density  $\rho_i = \rho\Theta_i$  of this extensive value and its transfer velocity  $\mathbf{v}_i$ . The transfer concepts extraneous to classic thermodynamics find thereby their realization in thermokinetics

Using the thermokinetic body of mathematics applicable for the investigation of processes with any irreversibility degree allows posing the issue of establishing general behavior of non-static energy conversion processes and thus enabling a synthesis of the theory of irreversible processes (TIP) with engineering thermodynamics dealing with the energy conversion process in heat engines.

This chapter highlights the new results in the theory of heat and non-heat, cyclic and non-cyclic machines, direct action machines and heat pumps obtained when applying the thermokinetic methods to them. One more step will thereby be done toward the creation of the unified theory of real processes.

### **18.1. Interrelation between Energy Transfer and Conversion Processes**

Classic thermodynamics, having time excluded from its equations, did not consider the processes of energy and its carriers transfer. Therefore the issue regarding unity of energy transfer and conversion processes could not arise in its depths. N. Umov was the first (1873) who paid attention to that relation and stated the energy conservation law (2.4.6) for mechanical processes rather as a consequence of energy transfer across the system borders than as a result of energy disappearing in some points of space and appearing in others. It remained unanswered, however, what was the “transfer substrate” in that case – either the material energy carriers attributed to the extensive values  $\Theta_i$  category or the intensive values  $\psi_i$  as analogs of mechanical stresses. Thermokinetics gives an answer to this question. According to (2.4.6) and (2.4.10) the flux of any  $i^{\text{th}}$  form of en-

ergy is expressed as the product of the intensive measure of motion – the generalized potential  $\psi_i$  – and the energy carrier flux  $\mathbf{J}_i$  that is defined, in its turn, as the product of the extensive measure of motion  $\Theta_i$  of this particular kind being transferred and the velocity  $\mathbf{v}_i$  of its transfer in space. This flux density  $\mathbf{j}_i$  is accordingly expressed as the product of the density  $\rho_i = \rho\Theta_i$  of this extensive value and its transfer velocity  $\mathbf{v}_i$ . The transfer concepts extraneous to classic thermodynamics find thereby their realization in thermokinetics.

Furthermore, thermokinetics allows easily distinguishing between the energy *transfer* processes (within the same form) and the energy *conversion* processes (from some form into another). With this purpose in mind let us consider a system with an arbitrary volume of  $V$  wherein a steady process of converting the  $i^{\text{th}}$  energy form into the  $j^{\text{th}}$  one is being realized. As shown in Chapter 2, this process is described by the second sum in the equation of energy conversion in the form (2.2.5), which terms characterize the capacity of energy conversion processes in the system.

The terms of this sum may be endowed with a more conventional form if taking into consideration that the redistribution processes correspond to the expansion of  $\nabla \cdot (\psi_i \mathbf{j}_i^e)$  into the (2.4.6) given that  $\nabla \cdot \mathbf{j}_i^e = 0$ . For the system as a whole this condition becomes  $\int \nabla \cdot \mathbf{j}_i^e dV = 0$ . Changing in this expression from the space integral to the integral  $\int \mathbf{j}_i^e \cdot \mathbf{n} df = 0$  taken through the closed surface  $f$  of the system gives that at  $\mathbf{j}_i^e \neq 0$  the said condition indicates the parts  $f'$  and  $f''$  existing on this surface with the opposite sign of the  $\mathbf{j}_i^e \cdot \mathbf{n}$  product, i.e. the flows  $\mathbf{j}_i'$  and  $\mathbf{j}_i''$  existing as entering the system and leaving it, respectively. In this case

$$\int \mathbf{j}_i \cdot \mathbf{n} df = \int \mathbf{j}_i' \cdot \mathbf{n} df' + \int \mathbf{j}_i'' \cdot \mathbf{n} df'' = J_i'' - J_i' = 0, \quad (18.1.1)$$

where  $J_i' = \int \mathbf{j}_i' \cdot \mathbf{n} df' \leq 0$  and  $J_i'' = \int \mathbf{j}_i'' \cdot \mathbf{n} df'' \geq 0$  – flows (flow rates) of energy carrier at the system input and output, respectively.

Thus in balance equation (2.5.3) the external component of the flow  $\mathbf{J}_i^e$  caused by the useful external work  $W^e$  done may be distinguished from the relaxation component  $\mathbf{J}_i'$  by the conservation of the energy carrier flow rates  $J_i'$  and  $J_i''$  at the system input and output. Representing in (2.4.7) the bulk element  $dV$  covered by the flow  $\mathbf{j}_i^e$  as a product of its cross section vector element  $d\mathbf{f}$  normal to the flow and the normal element  $d\mathbf{n}$  ( $dV = d\mathbf{f} \cdot d\mathbf{n}$ ) and also considering that in a steady flow  $(d\mathbf{n} \cdot \nabla)\psi_i = d\psi_i$  one may derive instead of the addend in (2.4.7):

$$N_i = \int (\int \mathbf{j}_i^e \cdot d\mathbf{f}) d\psi_i = - \int J_i^e d\psi_i = J_i^e (\psi_i' - \psi_i''), \quad (18.1.2)$$

where  $J_i^e = -\int \mathbf{j}_i^e \cdot d\mathbf{f} = J_i'' = -|\mathbf{J}_i'|$  – external “transit” flow of energy carrier crossing the system and remaining unvaried in value;  $\psi_i'$ ,  $\psi_i''$  – input and output potentials of energy carrier, respectively.

Thus the useful component is associated with the “transit” flow of energy carrier  $J_i^e$  which crosses the system with its value invariable. This statement may be instantiated by an electric machine where the input current is known to be equal to the output one. This is equally evident for a cyclic heat engine, too (Fig. 3.1), since in any cycle the entropy rise with the heat supply  $\Delta S_{1-2}$  is numerically equal to the entropy decline  $\Delta S_{2-1}$  with the heat rejected to heat sink. Therefore, at steady conditions the entropy flow rates  $J_s^e = \Delta S/\Delta t$  at the system input and output are as well equal. This is the circumstance that was foundational for S. Carnot to compare heat engine with a mill-wheel (hydraulic machine).

As follows from the aforementioned, the condition necessary to provide the conversion of some  $i^{\text{th}}$  energy form consists in the availability within the energy converting system an adequate energy carrier flow  $J_i^e$  crossing the areas with a various value of the generalized potential  $\Psi_i$ . For heat engines this is the entropy flow  $J_s^e$  from heat well with a temperature of  $T'$  to heat sink with a temperature of  $T''$ ; for electric machines – the electric current  $J_e^e$  associated with the electric potential differential  $\Delta\phi$ ; for concentration elements – the substance flow  $J_k^e$  crossing the borders of a system with different values of chemical potential; for mechanical engines – the gas or liquid flow between the zones with different values of enthalpy or pressure, etc. This distinguishing feature of the energy conversion processes, viz. transfer of a corresponding thermostatic value  $\Theta_i$  in the field of the  $X_i$  forces, is characteristic for micro-heterogeneous systems, too. In fact, a flow proper of some value across the borders of a system implies there are “flow-out” and “flow-into” zones in the system, i.e. subsystems reversing their properties in the course of energy conversion. These may be electrons and “holes” in semiconductors, positive and negative ions in electrolytes, opposite charges or poles of electric and magnetic dipoles, bulk elements shifting in opposite directions in bodies under deformation, etc.

This means that any system taking part in energy conversion process (either a source of technically fit energy, or the converting device proper, or the work object, or whatever else) should always be considered as an extended (heterogeneous) system, which different parts reverse their state. Such state variations are, in the broadest sense, that “compensation” for the energy conversion process, which necessity R. Clausius advocated.

Expression (18.1.2) is valid for both the  $i^{\text{th}}$  (being converted) and the  $j^{\text{th}}$  (having been converted) forms of energy. This means that any energy converting device (both cyclic and non-cyclic) is a system “transfused” with the energy-carrier flows of both “being-converted”  $\mathbf{J}_i$  and “having-

been-converted”  $J_j$  forms of energy. Such a “two-flow” system in electrical engineering is represented as a “four-terminal” network in electrical engineering and radio-engineering, i.e. a device with two pairs of input and output terminals. For clearness, an electrical “equivalent circuit” to an energy converting device is shown in Fig. 18.1.

The energy converting device depicted on this figure (central part) looks like being “transfused” with two different-kind flows of the energy carriers  $J_i$  and  $J_j$ . It is emphasized thereby that this device interacts with not just one, but two objects – *the source of technically fit energy (inergy)* and *the work object*. The principal distinction of a four-terminal network from the heat engine concept adopted in thermostatics as a set of heat well, working medium and heat sink is that the energy converting device (working medium analog) in the four-terminal network contacts two “extended” systems, each being non-equilibrium and including energy carrier wells and sinks (similar to the extended system). The function of the energy converting device in such a circuit is using the spatial heterogeneity in some material objects (*inergy source*) in order to create an artificial heterogeneity in other ones (work object).

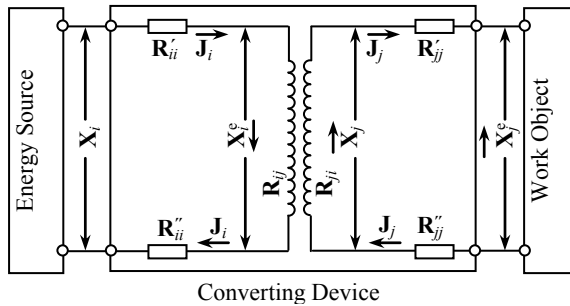


Fig.18.1. Electrical Equivalent Circuit to energy Converting Device

The functional division of the material objects participating in the energy conversion process stresses the *inseparable unity of the energy transfer and conversion processes* and provides the necessary generality in posing the issue on the thermodynamic perfection of the energy conversion process in heat and non-heat, cyclic and non-cyclic engines.

Such an approach is extremely important since the wells and the sinks of whatever source of energy can not be distinguished in nature with the same easiness as the heat wells and heat sinks. It is very difficult to distinguish the energy wells and sinks in such media as, e.g. homogeneous chemically reacting mixture, polarized or magnetized media, dissociated gases, deformed elastic bodies, etc. Nevertheless, those are known to be able to do useful work like the discontinuous systems. Sensing them as a

non-equilibrium single whole promotes the formation of a correct world outlook and the comprehension that all man-used energy sources, without exception, ultimately belong to only the environment and are caused by environmental spatial heterogeneity. This implies not just a possibility, but also an inevitability of using the environmental energy. The apparent contradiction of this conclusion with classic thermodynamics (its second law) that excludes the usage of the environmental heat is caused by just the fact that classic thermodynamics interprets the environment simplistically as something homogeneous. It is this environment that embodies the Ostvald-proposed concept of perpetual motion of the second kind as a heat engine using the practically inexhaustible heat well of the world ocean. Now, when power installations exist using the temperature difference between the surface and subsurface oceanic layers, i.e. the part of this indeed inexhaustible heat well, the narrowness of equilibrium thermodynamics in posing problems and drawing conclusions is undeniable.

## 18.2. Universal Index of Energy Converters' Perfection

The necessity to have both wells and sinks of entropy, charge, substance, momentum, etc. ensuing from (18.1.2) once again emphasizes the flexibility of the law of excluded perpetual motion of the second kind. This statement results in a possibility for each of the energy converting devices to be estimated by the process power  $N_i$  related to the energy flow at the inlet to the energy converter  $J_e'$ :

$$\eta_i = N_i / J_e' = N_i = 1 - \bar{\psi}_i'' / \bar{\psi}_i', \quad (18.2.1)$$

where  $\bar{\psi}_i'$ ,  $\bar{\psi}_i''$  – mean-integral values of the generalized potential at the device inlet and outlet.

This index refers to the so-called “absolute efficiencies” class. According to this expression the absolute efficiency characterizes the convertibility degree of the energy supplied from some energy well. This degree is defined by exclusively the relation between the mean values of a corresponding generalized potential and, providing this relation is constant, does not depend on the working medium properties, design and other characteristics of the energy converting system. Since energy wells with a potential of  $\bar{\psi}_i' = \infty$  or energy sinks with a potential of  $\bar{\psi}_i'' = 0$  are physically unfeasible, the 100% absolute efficiency is unattainable in even reversible processes. This verdict generalizes the Carnot theorem known for ideal heat engines confirming once again the conclusion that the laws of heat conversion stated by thermodynamics are just a particular case of the universal laws of nature valid for any forms of energy.

Let us now show that expression (18.2.1) is valid for cyclic heat engines, too. To do so, let us interrelate the so-called “mean-thermodynamic” temperatures  $\bar{T}_1$  and  $\bar{T}_2$  in the heat absorption and rejection processes with the mean-integral temperatures  $T_s'$  and  $T_s''$  of entropy flows at the device inlet and outlet. If  $\Delta S_1$  and  $\Delta S_2$  characterize the variations of the working medium entropy with the heats absorption and rejection  $Q_1$  and  $Q_2$  in some cycle, while  $\Delta t_1$  and  $\Delta t_2$  – duration of these processes, then the total flows of heat  $J_q'$  and  $J_q''$  and entropy  $J_s'$  and  $J_s''$  will be defined as:

$$J_q' = Q_1/\Delta t_1; J_q'' = Q_2/\Delta t_2; \quad (18.2.2)$$

$$J_s' = \Delta S_1/\Delta t_1; J_s'' = \Delta S_2/\Delta t_2. \quad (18.2.3)$$

Considering the relationship between the flows of heat and entropy as  $J_q = T_s J_s$  gives:

$$\bar{T}_1 = Q_1/\Delta S_1 = J_q'/J_s' = T_s', \quad (18.2.4)$$

$$\bar{T}_2 = Q_2/\Delta S_2 = J_q''/J_s'' = T_s''. \quad (18.2.5)$$

The identity of the temperatures averaged over the time of heat supply to the working medium in a heat exchanger to the temperatures averaged over the heat exchange surface allows deriving the thermal efficiency of an arbitrary cycle in terms of the heat flow parameters:

$$\eta_t = 1 - Q_2/Q_1 = 1 - T_2/T_1 = 1 - \bar{T}_s''/\bar{T}_s'. \quad (18.2.6)$$

Then

$$J_s' = J_q'/T_s' = J_s'' = J_q''/T_s''. \quad (15.2.7)$$

Thus marking the border of the energy converting device along the surface of heat exchange with the heat well and heat sink the operation of the cyclic heat engine may be reduced to the operation of a direct-heat-conversion machine with the same theoretical power  $N^e$  :

$$N^e = J_q' \eta_t = J_s' (T_s' - T_s'') = J_s' \Delta T_s, \quad (18.2.8)$$

where  $\Delta T_s = T_s' - T_s''$  – motive force of the heat transfer and conversion process defined by the energy well and sink parameters.

The unified expression of absolute efficiencies for heat and non-heat, cyclic and non-cyclic engines (see 18.2.1) shows that this value depends on neither a kind of the energy being converted and design of the energy converting device, nor on its working medium nature or parameters.

Therefore the value  $\eta_i$ , as well as  $\eta_i$ , strictly speaking should not at all be termed as “engine efficiency”. This value is defined by exclusively the parameters of the “hot” and “cold” energy well on the border with the working medium, i.e. by the energy flow parameters, but not the properties of the engine as itself. In other words, the “absolute efficiencies”, including the “thermal”, “internal”, “effective”, “electrical”, “enthalpy”, etc. efficiencies widely used in analysis of heat power units characterize rather the capabilities provided by nature due to its intrinsic spatial heterogeneity in dispensing of whatever intensive property. These efficiencies characterize just the maximal “convertibility degree” of a particular energy form, which is attained in the same machine with the quasi-static nature of the processes involved therein (when all the processes are “reversible”). According to the Carnot theorem this efficiency does not depend anymore on the working medium properties within the energy converting device, i.e. relates to some abstract (idealized) machine naturally not occurring. Since all reversible processes are infinitely slow running, the power of such a machine is infinitesimal. Therefore in thermokinetics dealing with real processes and machines we will be avoiding to apply the term “efficiency” to the value  $\eta_i$  terming it rather “energy convertibility degree”.

The so-called “relative” efficiencies have other meaning. In classic thermodynamics this notion is introduced in order to estimate the perfection of particular processes in heat power engines, e.g. the working medium expansion processes. Such efficiencies mean the work  $W_i$  actually done in the process related to its theoretically possible value  $W_i'$  (A. Andrushchenko, 1985). These are the efficiencies (relative) all other disciplines operate except thermodynamics. For non-cyclic machines doing one kind of the useful work these efficiencies actually characterize the perfection degree of a machine (i.e. the losses therein). The fact that thermodynamics operates absolute efficiencies, whereas the other disciplines operate relative ones, has caused confusion time after time. Quite often lamentations have been raised for a low efficiency of heat power stations and up-to-60%-of-fuel heat “wasted” to the environment, whereas the efficiency of fuel cells, electric and many other machines reaches 90% and above. But for all that it has never occurred to the “complainants” that only several percents of the  $Q_2$  heat given away in excess of a certain minimum of  $Q_{2r}$  can be referred to the so-called “wasted heat loss” since the heat  $Q_{2r}$  is not a loss, but the *condition necessary to provide the energy conversion process as itself*.

To eliminate this misconception and provide a methodologically unified approach to the converters of any forms of energy, the concept of relative efficiency should be generalized to all kinds of the energy con-



verting devices. To this end let us consider the power ratio between the converter inlet  $N_j$  and outlet  $N_i$  :

$$\eta_N = N_j/N_i = X_j J_j^e / X_i J_i^e \leq 1 . \quad (18.2.9)$$

This expression is quite close by implication to the notion of relative internal efficiency of heat engines in classic thermodynamics and goes over into it after multiplication of the numerator and denominator in (18.2.1) by an arbitrary time span  $\Delta t$ . In this case the (18.2.1) numerator characterizes the useful work actually done by the machine  $W_i = X_j J_j^e \Delta t$ , while the denominator – its theoretically possible value  $W_i^t = X_i J_i^e \Delta t$ . We will be terming the (18.2.1) ratio a “power” efficiency of the energy converting device. It is this expression that ensues from the law of energy conservation in the form of (2.4.9) for a particular case of a single-target machine intended for the conversion of the  $i^{\text{th}}$  form of energy into the  $j^{\text{th}}$  one.

Let us show now that it is this efficiency that characterizes the thermodynamic perfection of a machine, i.e. the degree the machine implements those potentials the well of the technically adequate (ordered) energy provides for it. In fact, according to the principle of heat and work equivalency (see 2.1.1) the ordered work  $W^e$  done by a cyclic machine related to the algebraic sum of the heats  $dQ$  it receives at all stages of the cyclic process is always equal to unity. Relating this work to only that part of the heat  $Q_1$  which is taken from the “hot” well is, from a mathematical standpoint, an implicit technique, moreover, such one that is not always feasible for even the heat engines (in particular, for the processes where temperature rise cohabits with heat rejection). This even more concerns the non-heat engines where the energy wells and sinks occupies the same space (such are, in particular, polarized, magnetized, etc. bodies). At such conditions it is advisable to consider only the actual power of the machine  $N_j$  related to that theoretically possible; such a ratio being construed as the power efficiency (see 15.2.1).

Another advantage of the power efficiency lies in its applicability to the analysis of multi-functional machines implementing a simultaneous conversion of several kinds of energy. Further advantage of the power efficiency is its applicability to the same extent to both the direct cycles and the reverse ones, for which the relative efficiency loses its meaning because the power consumed in this process is more than theoretically required. Ultimately the power efficiency application makes machines more compatible in the degree of perfection of the processes running therein since it allows for losses of all kinds – both at the energy transfer from the well to the converting device and at the energy conversion in the device itself.

To show the non-triviality of this concept, let us compare the  $\eta_N$  with the so-called “*exergy efficiency of technical systems for energy and substance conversion*”  $\eta_{ex}$  (Brodiansky, 1991). The latter characterizes the ratio of outlet exergy flow to inlet exergy flow in the machine. The concept of *exergy* as a measure of system working capability relative to the environment is described in Chapter 2 above. For an “extended system” (as including wells and sinks of heat, substance, charge, etc.) the exergy becomes its state function. The exergy flows are equidimensional with power, which links the exergy and power efficiencies. However, the exergy efficiency is not always associated with the conversion of some kind of energy into other one due to the so-called “transit” exergy flows existing. Such is, e.g. the exergy of flow of some substance crossing the reactor and not participating in the chemical transformations therein. Therefore the exergy flow ratio does not yet characterize the effectiveness of the energy conversion in a machine. Besides, the exergy efficiency depends on the exergy value itself as it is commonly construed, i.e. on the reference point choice for some form of exergy or other. This makes the exergy efficiency ambiguous, which restricts the applicability of this working capability function in the efficiency analysis for power and process installations.

Representing the power efficiency in terms of the flows  $J_i^e$  and  $J_j^e$  referring exclusively to the energy conversion processes eliminates the shortcomings of the exergy efficiency. The further consideration will confirm the power efficiency is the concept that not only corresponds to its physical meaning, but also provides the most objective assessment of the thermodynamic effectiveness of any energy converters.

### **18.3. Kinetic Equations of Energy Conversion Processes. Antisymmetry of Relationships Therein**

As shown above, any device converting some  $i^{\text{th}}$  form of energy into the  $j^{\text{th}}$  one is a two-flow system, i.e. features energy carrier flows of both the energy being converted  $J_i$  and the energy having been converted  $J_j$ . The interrelation between flows  $J_i$  and  $J_j$  is a distinctive feature of the energy conversion processes. One can make sure such an interrelation exists if compare, based on the law of conservation of energy, the expressions of the energy being converted and having been converted:

$$N_i = N_i^A + N_i^e = N_j^A + N_j^e. \quad (18.3.1)$$

This relationship is an equation of balance between the power input to the machine and power output from the machine. According to this equation the power input  $N_i$  is consumed to overcome both the subscript-similar dissipation forces  $X_i$  and the “alien” forces  $X_j$ , i.e. is not only converted into other form of the useful energy  $N_i^e$ , but also partly dissipates on the input resistors (this loss is usually designated as  $N_i^d$ ). In its turn, the power  $N_j$  converted into the  $j^{\text{th}}$  form is also partly lost in the secondary equivalent circuit (Fig. 18.1) thereby reducing the output useful power  $N_j^e$  necessary to overcome the useful forces  $X_j^e$ . Since by the law of conservation of energy

$$N_i^e = X_i J_i^e = N_j^e = X_j J_j^e, \quad (18.3.2)$$

the flows  $J_i^e$  and  $J_j^e$  appears to be interrelated. This interrelation shows itself in the fact that each of the flows  $J_i$  and  $J_j$  appears to be dependant on both the active forces  $X_i$  and  $X_j$  acting in the system, i.e. the kinetic equations of the energy conversion process should be written a priori in the form of Onsager’s phenomenological laws (5.1.6):

$$J_i = L_{ij} X_i + L_{ij} X_j, \quad (18.3.3)$$

$$J_j = L_{ji} X_i + L_{jj} X_j. \quad (18.3.4)$$

The number of the phenomenological coefficients in these equations may be reduced by applying the reciprocity relationships to them. However, it is advisable to preliminarily make sure the reciprocity relationships (see 5.5.3) for the energy useful conversion processes bear invariably anti-symmetrical character. To this end let us take into account the difference in sign for the work done to the energy converting device (this work is negative according to the rule of signs in thermodynamics, i.e.  $dW_i = -X_i dZ_i < 0$ ) and the work done by this device to the work object  $dW_j = X_j dZ_j > 0$ . With the sign properly considered the exact differential of system exergy may be expressed as

$$dE = -X_i dZ_i + X_j dZ_j. \quad (18.3.5)$$

Repeating the same reasoning as described in paragraph 4.5 when deriving the reciprocity relationships, based on the properties of the inergy  $E$  exact differential, one comes to the anti-symmetrical reciprocity relationships:

$$(\partial J_i / \partial X_j) = -L_{ij} = (\partial J_j / \partial X_i) = L_{ji}. \quad (18.3.6)$$

This proof of the so-called Cazimir's reciprocity relationships differs from those earlier proposed (V. Etkin, 1993) by a particular simplicity and obviousness. The opposite sign of the works  $dW_i$  and  $dW_j$  taken into account results in kinetic equations (18.3.2), (18.3.3) taking the form:

$$J_i = L_{ij}X_i - L_{ji}X_j, \quad (18.3.7)$$

$$J_j = L_{ji}X_i - L_{jj}X_j. \quad (18.3.8)$$

The kinetic equations of such a character (with their terms having different signs) better correspond to the concept of phenomenological (experience-based) laws than initial equations (18.3.3)–(18.3.4). The primary energy carrier flow  $J_i$  (e.g. the current in the primary winding of a transformer) is commonly known to decrease as the forces  $X_j$  being overcome increase (with approach to “no-load” operation) or, on the contrary, to increase as these forces decrease (with approach to “short circuit” operation). Similarly, the secondary energy carrier flow (e.g. the current in the secondary winding of a transformer) is commonly known to increase as the supply voltage  $X_i$  increases and to decrease as the secondary circuit resistance and the  $X_j$  decrease.

The proof of the Cazimir's reciprocity relationships adduced here for reversible part of the energy conversion processes is based on the law of energy conservation and, therefore, valid whenever linear phenomenological laws (15.3.3) and (15.3.4) remain valid. This circumstance throws fresh light on the origin of the Cazimir's reciprocity relationships exposing the underneath meaning of the requirements for different parity of forces with respect to time inversion. In fact, for the dissipation forces not changing their signs with time inversion (i.e. for the so-called “ $\alpha$ -type forces”) the Onsager's symmetry conditions, as shown above, are valid. Whenever a part of these forces have the reversible character (i.e. refer to the “ $\beta$ -type forces”), the Onsager's reciprocity relationships give place to anti-symmetry conditions (15.3.5). At the same time the consideration endeavored here shows that the applicability of the Cazimir's relationships is not actually restricted to the different-parity forces ( $\alpha$  and  $\beta$ -type) case. In fact, let us assume dealing with energy conversion processes of purely dissipative character. Such are, in particular, thermal conductivity, electric conductivity, diffusion and viscous friction described by Fourier's, Ohm's, Fick's and Newton's laws and resulting in only the substance and energy transfer. In this case all terms of kinetic equation (4.4.1) describing vector phenomena have the same sign  $X_i \cdot J_i > 0$  defined by their contribution to dissipative function (5.3.3). In this case reciprocity relationships (4.5.4) defining value and sign of the phenomenological coefficients  $L_{ij}$  in linear kinetic equations (5.4.1) give invariably positive

values of the phenomenological coefficients  $L_{ij} > 0$  in these equations and result in Onsager's reciprocity relationships  $L_{ij} = L_{ji}$ .

So for linear transfer processes of a purely dissipative character the matrix of phenomenological coefficients is always symmetrical. However, if in a transfer process useful (reversible) energy conversions occur, i.e. work is done against whatever forces other than dissipation ones, the reciprocity relationships acquire other character. In this case phenomena of the "ascending diffusion" type (transfer of components toward their concentration increase), system ordering, etc. are observed. These processes lead to gradients or differences of temperature, pressure, concentration, electric potential, etc., i.e. to deviation of the system from the internal equilibrium state for some of its degrees of freedom, whereas the system in whole is tending toward equilibrium. As a matter of fact, this is the nature of all the so-called "superposition effects" the theory of irreversible processes deals with. As we will make sure hereafter, the effects of such a kind bear anti-dissipative character. The processes of useful conversion of the  $i^{\text{th}}$  form of energy into the  $j^{\text{th}}$  one in various machines apply to these effects, too. This substantially extends the applicability of the anti-symmetrical reciprocity relationships (V. Etkin, 1993).

Let us now elucidate what character the relationships between the phenomenological coefficients  $L_{ij}$  acquire in a more general case, when these coefficients are some functions of the related thermodynamic forces  $X_j$ , so that kinetic equations (15.3.5) and (15.3.7) are non-linear. Applying to them generalized reciprocity relationships (15.3.5) gives for this case:

$$(\partial J_j / \partial X_j) = L_{ij}(X_j) + \sum_{\mu} X_{\mu} (\partial L_{ij}(X_j) / \partial X_{\mu}) , \quad (18.3.9)$$

so the generalized reciprocity relationships become:

$$L_{ij}(X_j) + \sum_{\mu} X_{\mu} (\partial L_{ij} / \partial X_{\mu}) = L_{ji}(X_j) + \sum_{\mu} X_{\mu} (\partial L_{ji} / \partial X_{\mu}) .. \quad (18.3.10)$$

From this it follows that the Onsager-Cazimir's symmetry conditions  $L_{ij} = \pm L_{ji}$  apply to also those cases when the diagonal phenomenological coefficients

$$L_{ii} = L_{ij}(X_j), L_{jj} = L_{ji}(X_i), \quad (18.3.11)$$

i.e. are some functions of the forces associated with them, whereas only minor (non-diagonal) terms of the phenomenological laws characterizing the superposition effects are linear. In fact, if the non-diagonal coefficients  $L_{ij}, L_{ji}$  are constant, then all expressions within brackets in relationships (18.3.10) become zero. In other words, to meet the symmetry condi-

tions or non-symmetry ones, it is enough the non-diagonal terms in equations (18.3.7) and (18.3.8) responsible for the superposition effects to be linear. We have demonstrably instantiated this by the phenomena of cross diffusion and filtration of ideal gases thru the finite-thickness membrane.

It is a matter of interest to confirm the anti-symmetrical reciprocity relationships by specific examples of the useful energy conversion processes. As one of the examples, the thermoelectric generator (TEG) may be considered which operation is based on the Seebeck and Peltier thermoelectric effects. If the ends of different-type conductors  $A$  and  $B$  are connected and a current source or a load switched into the break of one of them, then in the formed thermo-circuit along with the Thomson's homogeneous effect (electric potential gradient generated along the dead conductor with heterogeneous temperature field) the so-called heterogeneous effects will be observed. One of them arises with the hot and cold junctions of the thermocouple maintained at different temperatures  $T_1$  and  $T_2 < T_1$ . It consists in the generation of the electromotive force  $X_e = -\Delta\phi$  proportional to the temperature difference  $X_q = -\Delta T = T_1 - T_2$  and reaching the maximum value in the absence of the electric current  $J_e$  (Haase, 1967):

$$(\Delta\phi/\Delta T)_{eT} = \varepsilon_{AB}/T \quad (J_e = 0), \quad (185.3.12)$$

where  $\varepsilon_{AB}$  – the so-called thermoelectric force in the thermo-circuit of conductors  $A$  and  $B$  depending on their nature and the mean temperature of the thermo-element  $T$ .

Another effect arises with the current  $J_e$  passed thru the junctions and consists in absorbing or releasing by the junction a Peltier heat which flow  $J_q$  is proportional to the current  $J_e$  and the junction temperature  $T$ :

$$J_q = \varepsilon_{AB} J_e T. \quad (18.3.13)$$

With the junctions of the thermo-circuit maintained at different temperatures, the electric current  $J_e$  generated will lead to the heat absorption  $J_q' = \varepsilon_{AB} J_e T_2$  in junction  $A$  and the heat release  $J_q'' = \varepsilon_{AB} J_e T_1$  in junction  $B$ . Then, in the absence of side processes, the thermo-element becomes similar to a cyclic heat engine with working medium being the free electrons circulating in the thermo-circuit. The dependence of the thermal conductivity  $\lambda$  and the electric conductivity  $\sigma_e$  of the thermo-circuit branches on the fields of temperatures along the conductors (and, thus, on the electric fields associated) makes the TEG phenomenological laws, strictly speaking, non-linear. However, the said non-linearity concentrates in their di-

agonal terms so that the TEG phenomenological laws become (Haase, 1967):

$$J_q = L_{qq}(X_q) X_q - L_{qe} X_e, \quad (18.3.14)$$

$$J_e = L_{eq} X_q - L_{ee}(X_e) X_e, \quad (18.3.15)$$

where  $L_{qq}(X_q)$ ,  $L_{ee}(X_e)$  – coefficients inverse to, respectively, thermal and electrical impedance of the thermo-circuit branches considered as a function of their mean-integral temperature;  $L_{qe}$ ,  $L_{eq}$  – cross phenomenological coefficients considered as constant. Here in equations (18.3.7) and (18.3.8) the circumstance is taken into account that with the voltage drop  $X_e$  at the TEG output the current  $J_e$  on the load and Peltier heat flow rise.

To make sure the anti-symmetry conditions  $L_{qe} = -L_{eq}$  for TEG are met also in the case the coefficients  $L_{qq}$  and  $L_{ee}$  depend on the associated forces, let us apply the differentiation process corresponding to the left side of equation (18.3.6) to equation (18.3.14). Allowing for constancy of  $L_{qq}(X_q)$  at  $X_q = \text{const}$  gives:

$$(\partial J_q / \partial X_e) = -L_{qe}. \quad (18.3.16)$$

The same with the (18.3.7) right side gives:

$$(\partial J_e / \partial X_q) = L_{eq}. \quad (18.3.17)$$

Thus, Cazimir's reciprocity relationships  $L_{eq} = -L_{qe}$  for TEG remain valid also with non-linear character of the main terms in equations (18.3.14) and (18.3.16).

A significant consequence from the anti-symmetry of phenomenological coefficients matrix for the useful energy conversion processes is the absence of limitations for the value of the cross phenomenological coefficients, which ensue in TIP from the condition of positive determinacy of their matrix (5.1.9). In fact, at  $L_{ij} = -L_{ji}$  condition (5.1.9) is met with any values of the coefficients  $L_{ij}$  and  $L_{ji}$ . As will be shown a little bit hereafter, this circumstance is of key importance since removes the limitations for efficiency, which is unusual to energy converting systems.

#### 18.4. Similarity Criteria for energy Converting Systems

The unity of phenomenological laws (18.3.7)-(18.3.8) describing different forms of energy conversion processes and their independence on machine hardware implementing such processes allows laying a founda-

tion to the similarity theory of linear energy converting systems. The math model of such a system includes, along with equations (18.3.7)-(18.3.8), the *uniqueness conditions* of processes under investigation. These conditions include:

a) conductivity  $L_{ij}$  or resistance  $R_{ij}$  coefficients ( $i, j = 1, 2$ ) characterizing the transport properties of the system (analog of the thermo-physical properties in the heat and mass transfer theory);

b) *boundary conditions* defined in this case by the values of motive forces at the current conditions  $X_i, X_j$ , or by the flow values at these conditions  $J_i, J_j$ ;

c) *initial conditions* defined by these force or flow values in “no-load” operation of the machine (at  $J_j = 0$ )  $X_{j0}, J_{i0}, J_{j0}$  and in “short circuit” operation (at  $X_j = 0$ )  $J_{ik}, J_{jk}$ . These uniqueness conditions allow forming a number of dimensionless criteria of energy converting systems similarity. Equations (18.3.7)-(18.3.8) are more practical to be expressed in terms of the resistance coefficients  $R_{ij}$  in the form:

$$X_i = R_{ii} J_j - R_{ij} J_j ; \quad (18.4.1)$$

$$X_j = R_{ji} J_j - R_{jj} J_j . \quad (18.4.2)$$

Let us consider these equations jointly with the uniqueness conditions. Assuming  $J_{j0} = 0, X_i = X_{i0}, X_j = X_{j0}$  they can be derived as:

$$X_{i0}/X_{j0} = R_{ij}/R_{ii} ; \quad J_j = X_{j0}/R_{ji} ; \quad J_j = (X_j - X_{j0})/R_{jj} . \quad (18.4.3)$$

Similarly for “short circuit” conditions ( $X_j = 0, J_j = J_{jk}, J_j = J_{jk}$ ) equation (18.4.2) becomes:

$$J_{jk}/J_{ik} = R_{ji} /R_{jj} . \quad (18.4.4)$$

Substituting equations (18.4.1) and (18.4.2) in power efficiency expression (18.2.9) and making a number of transformations using relationships (18.4.3) and (18.4.4) gives:

$$\eta_N = (X_j/X_{j0})/[1 + R_{ii} R_{ij}/R_{ji}^2 (1 - X_j/X_{j0})]. \quad (18.4.5)$$

This equation allows reducing the uniqueness conditions characterizing the transport properties of the energy machine to a one dimensionless complex:

$$\Phi = R_{ji}^2 /R_{ii} R_{jj} . \quad (18.4.6)$$



This complex is similar to the relationship between active and reactive resistances known in radio engineering as tuned-circuit Q-factor and coincides (accurate up to a temperature factor) with the “torque-to-weight ratio”  $\Phi$  introduced by A. Yoffe as a generalized characteristic of thermoelectric generators (TEG). Therefore it was termed as a *good quality criterion of machine* (V. Etkin, 1990). Its value ranges from zero to infinity ( $0 < \Phi < \infty$ ) increasing with decrease of the “active” resistances  $R_{ii}$  and  $R_{jj}$  (from the dissipation forces) and increase of the “reactive” resistances  $R_{ji}$  (from the useful forces). Like the thermal resistances these ones depend on the transport properties of the system (cross-sections and lengths of the heat, substance, charge, etc. transfer lines, properties of the materials applied, transport factors, etc.), i.e., ultimately, on the design perfection of the machine indirectly depending on also its manufacturing expenditures. Based on this, the above criterion could also be termed as a *criterion of design perfection of machine*.

Other dimensionless criterion can be composed of boundary conditions defined by the values of the forces  $X_j$ ,  $X_{j_0}$  or flows  $J_j$ ,  $J_{j_0}$ :

$$B = J_j / J_{j_0} = 1 - X_j / X_{j_0}. \quad (18.4.7)$$

This criterion depends on exclusively the load to the machine (“load current”) and ranges from zero at no-load conditions ( $J_j = 0$ ) up to unity at short circuit conditions ( $X_j = 0$ ). Therefore it was termed as a *load criterion of machine* (V. Etkin, 1990, 1991).

Using these criteria expression (18.4.5) can be formed as a *criterion equation of energy conversion process*:

$$\eta_N = (1 - B)/(1 + 1/B\Phi). \quad (18.4.8)$$

This equation determines the dependence of the thermodynamic criterion of machine perfection upon machine load  $B$  at invariable parameters of the technically fit energy source. According to it *relative efficiency is the same for any linear energy converter at similar conditions ( $B, \Phi = idem$ )*. This statement is reasonable to be called for easy reference as the **similarity principle** of energy conversion processes.

Thereby one more step has been made on the way to approach the thermodynamic assessment of technical system efficiency to reality.

## 18.5. Universal Load Characteristics of energy Converters

Like the theory of heat exchange processes similarity, criterion equation of energy conversion processes (18.4.8) allows extending the results of efficiency investigation from some technical systems to other ones (insufficiently explored). To do so, it is advisable to build based on criterion equation (18.4.8) a generalized load characteristic of linear energy converting systems. Such a characteristic is plotted on Fig.18.2. Solid lines show here the power efficiency of the machine  $\eta_N$  plotted against the load criterion  $B$  for different values of the Q-criterion  $\Phi$ , while dotted lines – the output power  $N_j$  plotted against the load. As follows from the figure, in the absence of energy losses ( $\Phi = \infty$ ) and with quasi-static character of its conversion ( $B \rightarrow 0$ ) the machine efficiency reaches, as should be expected, unity. However, in all other cases the power efficiency becomes zero twice: in “no-load” ( $B = 0, J_j = 0$ ) and “short circuit” ( $B = 1, X_j = 0$ ) operations. This ensues from taking into account, along with the irreversible power interchange and friction, also various “leaks”<sup>1)</sup> of power occurring in also “no-load” operation of the machine, in particular, its auxiliary power. With the loads growing and the operation withdrawing from “no-load” conditions the efficiency rises and reaches maximum at a definite load. The efficiency maximums then lie on the same line connecting the operating conditions with “zero” output power ( $B = 0, \eta_N = 1$  и  $B = 0,5, \eta_N = 0$ ). The efficiency maximums appeared are explained by varying relationship between the rates of useful and dissipative energy conversions in the system and show that all types of energy converters have the most economical loads usually adopted as *nominal*.

To find the nominal loads  $B_n$ , let us set the derivative of (18.4.8) with respect to  $B$  equal to zero. Some transformations give:

$$B_n = (\sqrt{1 + \Phi} - 1) / \Phi. \quad (18.5.1)$$

According to this expression the power efficiency maximums lie on the same line connecting the points with the load  $B = 0.5$  and the efficiency  $\eta_N = 1$ . The max efficiency value depends in this case on exclusively the Q-criterion value. In fact, substituting (15.5.1) into criterion equation (15.4.8) gives after simple transformations:

$$\eta_N^{\max} = (\sqrt{1 + \Phi} - 1) / (\sqrt{1 + \Phi} + 1). \quad (18.5.2)$$

---

<sup>1)</sup> This loss can not be taken into account by traditionally introducing the constant relative efficiencies of work-doing processes since this loss is equal to zero in “no-load” operation.

As can be seen, with the  $\Phi$ -factor of the machine rising (by additional investments as well), the nominal operating conditions shift toward decreasing loads. However, on partial loads (below nominal) the power efficiency drops in this case even more abruptly. In this respect the deductions of thermokinetics also comply with a known provision that the operation of high-efficiency power machines on partial loads is inadvisable. To clarify how the load impacts on the output power of a machine, let us substitute (15.4.8) into the relationship  $N_j = N_i \eta_N$  :

$$N_j = X_{j0} J_{jk} B(1 - B) . \quad (18.5.3)$$

Since at  $B = 0.5$  the power  $N_j$  is maximal ( $N_j = N_j^{max}$ ), the value  $X_{j0} J_{jk} = 4 N_j$ , and instead of (18.5.3) one can write

$$N_j / N_j^{max} = 4 B(1 - B) . \quad (18.5.4)$$

This plot is also shown on Fig.18.2 with dotted line. From this it follows that at the efficiency  $\eta_N = 1$  the output power of any heat engine is equal to zero due to the absence of heat exchange between the heat well and working medium and reaches maximum at a relative load of  $B = 0.5$ . The efficiency of the engine corresponding to these loads can be found by substituting this load value into (18.4.8):

$$\eta_{(N=\max)} = 1/(2 + 4/\Phi) . \quad (18.5.5)$$

According to this expression the power efficiency of linear energy converters at max power conditions does not exceed 50 % for all forms of energy. For all that the difference in efficiencies of machines with different  $\Phi$ -factors is leveling off with approaching the max-output power-operating conditions and may become practically indistinguishable. This fact reveals lack of prospects in pursuing high efficiencies for power machines intended for peak-load or power-augmentation operations.

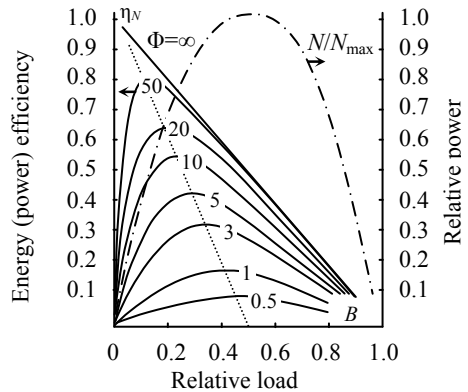


Fig.18.2. Universal Load Characteristics of Linear Systems

Fig.18.2 also shows that with the  $\Phi$ -factor of a machine rising, the dependence of its efficiency on load grows more perceptible, while the op-

erating conditions of max efficiency and max output power are more and more drifting apart.

Other important conclusion from loading characteristics is possibility of a finding of criterion of good quality (constructibility) of installation  $F$  by maximum position moshchnostnogo efficiency  $\eta_N$ . Equating zero derivative of expression (185.4.8), we will find:

$$\Phi = (1 - 2B_{\text{opt}}) / B_{\text{opt}}^2. \quad (18.5.6)$$

where  $B_{\text{opt}}$  - the optimum loading corresponding to a maximum of efficiency  $\eta_N$ .

The indirect confirmation of the anti-symmetry of reciprocity relationships is another significant conclusion from the load characteristics. In fact, if the Onsager's symmetry conditions were valid for energy converting machines, then they would engender known limitations for the relationship of diagonal and non-diagonal phenomenological coefficients  $L_{ij}^2 / L_{ii} L_{jj} \leq 1$  or  $\Phi = R_{ji}^2 / R_{ii} R_{jj} \leq 1$  as based on the positive determinacy of phenomenological coefficients matrix (5.1.9). In accordance with Fig.18.2 this means that the exergy efficiency of any energy converters can not exceed  $\sim 17.5\%$  as a limit. Meantime a lot of machines are known with this efficiency exceeding the limit. The said contradiction is eliminated if  $L_{ij} = -L_{ji}$  since in this case condition (5.1.9) means just the requirement these coefficients to be positive ( $L_{ii} L_{jj} \geq 0$ ).

The universal load characteristics are very convenient when comparing machines of different types for choosing the most challenging of them. Since such an assessment depends on the load of a machine ranging considerably in operation, the comparison needs the load characteristics to be known otherwise being insufficient. Let us show this by example of a hydrazine-oxygen electrochemical current generator (ECG). When operating this fuel cell, a no-load voltage (EMF) was obtained as  $X_{j_0} = 1.6$  V which decreases with load growth and becomes  $X_j = 0.85$  V at a power of  $N_j = 2$  kW. Fuel utilization factor and oxidant utilization factor for this unit are  $\eta_f = 0.8$  and  $\eta_{\text{ox}} = 0.9$ , respectively (B. Nesterov and others, 1980). To find the ECG power efficiency, let us first calculate the fuel element relative load  $B = 1 - X_j / X_{j_0} = 1 - 0.85 / 1.6 = 0.47$ . For ideal ECG (with the  $\Phi = \infty$ ) under such a load according to Fig.15.2  $\eta_N$  does not exceed 0.51. Allowing for the mean factor of reagents utilization as  $\eta_r = 0.85$  gives the effective efficiency for this generator  $\eta_e = \eta_N \eta_r = 0.51 \cdot 0.85 = 0.43$ . Detailed calculations with an exergy flow balance analysis give for this ECG the exergy efficiency  $\eta_{\text{ex}} = 0.41$  (V. Etkin, 1991), i.e. quite close to  $\eta_e$ . At the same time such a proximate analysis reveals the importance of considering the loads to machines when investigating how far they are challenging. Should in the example considered the ECG effec-

tiveness be estimated thru the max power efficiency  $\eta_N \cong 0.85$ , the situation would be cardinally outweighed on its side.

### 18.6. Similarity of Load Characteristics for Real Machines

It is a matter of interest to confirm the similarity of load characteristics for a number of different-type energy converters. As one of the examples, let us consider a space-based propulsion system (SBP). For spacecrafts moving in the absence of air drag and gravity the useful work means the acceleration  $d\mathbf{v}/dt$  of a spacecraft with the mass  $M$  under the thrust  $\mathbf{R}$ . This thrust is defined by a known expression (Favorsky and others, 1970):

$$\mathbf{R} = G_m \mathbf{w} + F_c (p_c - p_o) \mathbf{n} = G_m \mathbf{w}_s = R_y \mathbf{g} G_m, \quad (18.6.1)$$

where  $G_m$  – gas flow thru jet nozzle, kg/s;  $\mathbf{w}$ ,  $\mathbf{w}_{eq}$  – true and equivalent gas outflow velocity, respectively;  $p_n$ ,  $p_o$  – pressure of combustion products at the nozzle outlet and outside in the environment, respectively,  $\text{N/m}^2$ ;  $\mathbf{R}_s$ ,  $\mathbf{g}$  – specific thrust (specific impulse) of the jet engine and gravitational acceleration, respectively.

In the general case of flights in the atmosphere or gravity field the part  $N_j^d$  of the converted power  $N_j$  works against the environmental resistance forces. Here the useful effect is deemed as the movement of a flying vehicle and the  $N_j$  value defined as the scalar product of the thrust  $\mathbf{R}$  by the distance covered per unit time under this thrust. For spacecrafts taking off from the orbit of the Earth with the starting orbital velocity  $\mathbf{v}_o$  this distance is obviously equal to the velocity of spacecraft movement relative to the starting coordinate system  $\mathbf{v}_k = \mathbf{v} - \mathbf{v}_o$  since at  $\mathbf{v} = \mathbf{v}_o$  no work is done:

$$N_j = \mathbf{R} \cdot (\mathbf{v} - \mathbf{v}_o). \quad (18.6.2)$$

This expression is applicable also for the engines correcting the satellite orbit and for the flying vehicles taking off from the Earth's surface ( $\mathbf{v}_o = 0$ ). Taking into account that the vectors  $\mathbf{R}$  and  $\mathbf{v}$  are anti-parallel (so that the problem may be considered as one-dimensional) the output power  $N_j$  may be represented as the product of the scalar thermodynamic force  $X_j = |\mathbf{R}| = R$  as a motive force or acceleration of the vehicle by the scalar flow  $J_j = |\mathbf{v} - \mathbf{v}_o| = v - v_o$  as a generalized velocity of the movement process.

To find the flows and forces of the energy form being converted, let us apply to the first law of thermodynamics for unit mass of moving

gases. Under this law, if the processes in combustors and nozzles are running at adiabatic conditions, the specific useful work of the vehicle movement relative to the starting coordinate system is defined by the difference in enthalpy of the combustion products deceleration between the combustor inlet  $h_c^* = h_c + \mathbf{v}_c^2/2$  and the nozzle outlet  $h_k^* = h_k + \mathbf{v}_k^2/2$ . According to this the power input to the engine is defined as:

$$N_i = G_m (h_c^* - h_k^*) . \quad (18.6.3)$$

This expression may be also represented in the form of the product of the scalar gas flow  $J_i = G_m$  as a generalized rate of the process by the scalar thermodynamic force  $X_i = -\Delta h^*$ . The difference of enthalpies  $\Delta h = h_k - h_c$  is known to define the theoretical velocity  $\mathbf{w}_t$  of gas outflow from the nozzle ( $\mathbf{w}_t^2/2 = h_k - h_c$ ) which relates to the true gas outflow velocity  $\mathbf{w}$  thru the relative internal efficiency  $\eta_{oi} = \mathbf{w}^2/\mathbf{w}_t^2$ . Taking into account that for space engines the equivalent gas outflow velocity from nozzles  $\mathbf{w}_{eq}$  is substantially equal to the true outflow velocity  $\mathbf{w}$ , while the absolute outflow velocity for working medium at the nozzle outlet in the starting coordinate system  $\mathbf{v}_c$  is equal to the difference between  $\mathbf{w}$  and the velocity of the flying vehicle in this coordinate system  $\mathbf{v}$ , the value  $X_i$  may be represented as:

$$h_k^* - h_c^* = \mathbf{w} \cdot (\mathbf{v} - \mathbf{v}_o) + (1/\eta_{oi} - 1) \mathbf{w}^2/2 . \quad (18.6.4)$$

The augend on the right side of this equation defines the useful component of thermodynamic force  $X_i^e = \mathbf{w} \cdot (\mathbf{v} - \mathbf{v}_o)$  associated with the vehicle acceleration, while the addend – the dissipative component associated with the initial energy dissipation in the SBP combustors and nozzles (including losses caused by incomplete expansion, dissociation and ionization of working medium, as well as friction loss)  $X_i^r = (1/\eta_{oi} - 1)\mathbf{w}^2/2$ . The useful force component  $X_i^e = \mathbf{w} \cdot (\mathbf{v} - \mathbf{v}_o)$  is proportional to the flow  $J_j = |\mathbf{v} - \mathbf{v}_o|$  thru the proportionality factor  $-R_{ij} = |\mathbf{w}|$ , while the dissipative component – to squared velocity (and, consequently, squared flow  $G_m = J_i$ ). This causes non-linearity of the relationship  $X_i = X_i(J_i)$ . However, this non-linearity is concentrated in the diagonal term that may be represented as  $X_i^r = R_{ii}G_m = [(1/\eta_{oi} - 1)\mathbf{w}^2/2G]G_m$ , where the diagonal phenomenological resistance coefficient  $R_{ii} = (1/\eta_{oi} - 1)\mathbf{w}^2/2G_m = R_{ii}(G_m)$ , i.e. is a function of the flow associated.

Similarly, the thrust  $X_j = R$ , in the general case of flights in the atmosphere or gravity field, may be represented as a sum of the useful component  $X_j^e = Gw$  associated with the vehicle acceleration and proportional to the flow  $J_i = G_m$  thru the proportionality factor  $R_{ji} = w$  and the

dissipative component  $X_j'$  associated with the atmosphere resistance to be overcome and depending on the flight velocity  $J_j = |\mathbf{v} - \mathbf{v}_o|$ . This dependence is also non-linear, but may be represented in the pseudo-linear form  $R_{jj}(J_j)J_j$  thru the proportionality factor  $R_{jj}(J_j)$  depending on the velocity increment  $\Delta v$ .

Thus the SBP phenomenological laws may be expressed in informal variable as:

$$-\Delta h^* = R_{ii}(G_m) G_m - \mathbf{w} \cdot (\mathbf{v} - \mathbf{v}_o) , \quad (18.6.5)$$

$$R = w G_m - R_{jj}(\mathbf{v} - \mathbf{v}_o) . \quad (18.6.6)$$

Here the negative sign of the second term in equation (13.6.5) allows for the opposite direction of the force  $\mathbf{X}_i$  and the flight velocity  $\mathbf{v} - \mathbf{v}_o$ . In accordance with this equation at  $\Delta h^* = \text{const}$  increasing the flight velocity demands increasing the working medium flow, which is the reality. Similarly the negative sign of the second term in equation (18.6.6) allows for the fact that at the constant thrust and constant flow of working medium  $G$  increasing the flight velocity  $\mathbf{v} - \mathbf{v}_o$  demands increasing the propulsive jet velocity  $\mathbf{w}$ , which is quite natural, too. Such a character of the SBP phenomenological laws leads to the anti-symmetry of reciprocity relationships. In fact, applying relationships (18.3.5) to equations (18.6.5) and (18.6.6) gives:

$$(\partial X_i / \partial J_j) = -R_{ij} = (\partial X_j / \partial J_i) = R_{ji} = w . \quad (18.6.7)$$

The fact that the non-linear laws of mechanical energy forms conversion in SBP are quite within the frames of thermokinetics substantially expands its applicability and allows extending its analytical methods to complex mechanical systems, which seems to be quite important (Burdakov, 1985).

Now let us find the SBP power efficiency using the above-obtained expressions for input and output powers of the machine. Simplifying expression (15.6.4) as:

$$h_k^* - h_c^* = \mathbf{w}^2 / 2 \eta_{oi} + \mathbf{v}^2 / 2 , \quad (18.6.8)$$

gives that the SBP power efficiency  $\eta_N$  takes the form:

$$\eta_N = \mathbf{w} \cdot (\mathbf{v} - \mathbf{v}_o) / (\mathbf{w}^2 / 2 \eta_{oi} + \mathbf{v}^2 / 2) . \quad (18.6.9)$$

At  $\mathbf{v}_o = 0$  and  $\eta_{oi} = 1$  this relationship goes over into a known expression for the propulsion (thrust) efficiency (Alemasov, 1962). This differs from the SBP total efficiency by the velocity increment for the flight time

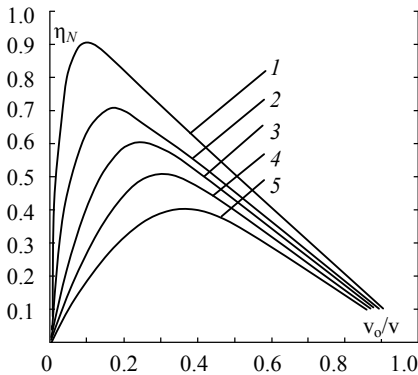
$(\mathbf{v} - \mathbf{v}_o)$  it features instead of the absolute flight velocity  $\mathbf{v}$  in the SBP total efficiency. Thereby it is taken into account that maintaining the flight velocity  $\mathbf{v} = \mathbf{v}_o$  in the absence of the air drag does not demand any work. Expression (15.6.2) can be reshaped to a more general form by introducing the relation  $B = v_o/v$  as the SBP load criterion:

$$\eta_N = 2B(1 - B)/[B^2(\mathbf{w}/\mathbf{v}_o)^2/2\eta_{oi} + \mathbf{v}_o/\mathbf{w}] . \quad (18.6.10)$$

The above relationship is correspondingly plotted on Fig.18.3. It is easy to see that its character completely corresponds to the universal load characteristics on Fig.18.2 despite the non-linearity of SBP phenomenological laws (18.6.5) and (18.6.6). Fig.18.3 shows that the machine efficiency as a function of the relative load  $B$  (flight relative velocity  $\mathbf{v}_o/\mathbf{v}$ ) becomes zero twice: at  $B = 0$  and  $B = 1$ . The first case corresponds to near-the-light speed flights when a further flight speed increment becomes impossible ( $J_j = J_{jk}$  – just like at “short-circuit” conditions). Such a situation is of theoretical interest for the spacecrafts with the solar sails (Favorsky and others, 1970), which thrust drops to zero as the flight speed is approaching the light speed.

The opposite case ( $B = 1$ ) applies to any spacecrafts at the moment they are taking off, when the flight speed is equal to the starting one ( $\mathbf{v} = \mathbf{v}_o$ ). With the flight speed increasing the efficiency curve reaches its peak value which position depends on the  $\mathbf{v}_o/\mathbf{w}$  ratio and the perfection degree of the internal processes in the engine.

As another example let us compare the individual characteristic of a thermionic energy converter (TEC) built based on the universal load



1, 2, 3, 4, 5 –  $\mathbf{R}_s/\mathbf{v}_o = 1.0; 0.5; 0.2; 0.15; 0.1$

Fig.18.3. Generalized Curves SBP Efficiency – Flight Speed

characteristic (Fig.18.2) for a known Q-criterion  $\Phi$  with the power and effective efficiency of one of such converters plotted experimentally against its output voltage  $\Delta\phi$  (M. Tribus, 1970). When investigating the TEC Q-criterion, we will proceed from the TEC characteristics, according to which the TEC effective efficiency  $\eta_e$  does not exceed 11% at the cathode and anode temperatures  $2,200^{\circ}\text{C}$  and  $30^{\circ}\text{C}$ , respectively. Proceeding from the fact that at these temperatures the theoretical efficiency of ideal TEC  $\eta_t^k \approx 0.88$  gives the



power efficiency  $\eta_N = 12.5\%$  corresponding to the above effective efficiency. In principle, this is enough to choose from the curves on Fig.18.2 and to plot a TEC individual load curve. To be able to compare it with the experimental curve of the effective efficiency  $\eta_e$  against the TEC output voltage, it is necessary to convert it into a generalized form of  $\eta_N = \eta_N(B)$ . This may be easily done by relating the TEC output voltage  $\Delta\phi$  to the “no-load” voltage (TEC EMF)  $\Delta\phi_0 = 0.9$  V since for the TEC  $B = 1 - \Delta\phi/\Delta\phi_0$ . The results of such a conversion are illustrated on Fig.18.4. Here the light dots denote the experimental values of effective efficiency, while the black dots – the experimental values of the TEC specific power. As follows from the figure, in general, the character of the curves  $\eta_N = \eta_N(B)$  and  $N = N(B)$  well complies with the universal load characteristics.

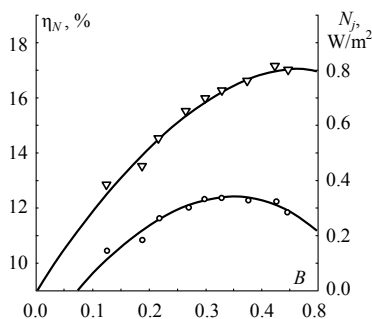


Fig.18.4. Load Characteristics of Thermionic energy Converters

The universal character of the load characteristics on Fig.18.2 may be further instantiated by the experimentally-found load characteristics of vortex-type gas energy separators based on the Ranque-Hilsch effect. The phenomenon of homogeneous gas energy separation into “cold” and “hot” flows known as the “vortex effect” or Ranque-Hilsch effect was discovered in 1933 by the French metallurgical engineer J. Ranque and then more thoroughly investigated by R. Hilsch in 1946. The vortex tube (VT), where the Ranque-Hilsch effect appears, is a smooth cylindrical or conical tube with one of the ends closed by a diaphragm having a central hole and the other end provided with a throttle having a size-controllable annular slot positioned around the tube periphery. The tube is equipped with tangential nozzles positioned mostly near the diaphragm. Compressed thermally homogeneous gas is fed thru the nozzles to the tube forming two vortices there drifting in the opposite directions inside the tube. One of them, peripheral, rotates with about constant rotational velocity  $\mathbf{v}_\tau = \boldsymbol{\omega} r = \text{const}$  (where  $\boldsymbol{\omega}$  – angular velocity;  $r$  – vortex current radius) and drifts toward the throttle leaving it notably heated if throttled down enough; while the other vortex, central, rotates by the laws of rigid body  $\mathbf{v}_\tau/r = \text{const}$  and drifts toward the diaphragm leaving it cooled. The cooling effect rate may reach  $(60-70)^\circ\text{C}$  and more, which causes a keen interest in the vortex effect from both theoreticians and empirics. Vast information is presently available on experimental investigation of this effect. Fig.18.5 demonstrates a piece of the most complete data of full-scale tests made on the vortex tube (Biruk,

1993). Here the dotted lines denote the separation factor  $\eta_T = 1 - T_h/T_c$  (where  $T_h, T_c$  – absolute temperatures of the “hot” and “cold” flows, respectively) plotted against the relative load of the machine defined by the cold air share  $\mu \equiv B$  for various ratios between the gas pressures upstream and downstream of the nozzle  $\pi = p_1/p_2 = 2, 5, 7$ . In that case the relative load value ranged from zero (at “no-load”) to unity (“short circuit” analog). The solid lines on the figure denote the vortex tube “cooling capacity”  $\mu\eta_T$  related to primary gas flow unit and measured by the product of cold air share  $\mu$  and the temperature separation factor  $\eta_T$  and plotted against the load  $B \equiv \mu$ . As this value is nothing else but the outlet gas flow exergy per gas flow unit, the curves on Fig.18.5, at  $\pi$  given, are nothing else but the individual load characteristics of the vortex tube plotted to a certain scale. It can be easily seen that the curves  $\eta_T = \eta_T(B)$  and  $\mu\eta_T = \mu\eta_T(B)$  in their character satisfactorily reproduce the universal load characteristics of linear energy converting systems  $\eta_N = \eta_N(B)$  and  $N = N(B)$  despite the non-linearity of gas expansion in the nozzles of the vortex separators. It is significant that with increasing  $\pi$  ( $\Phi$ -criterion analog) the peak values of the separator economical efficiency  $\eta_T$  drift toward the relative loads  $B = \mu$  reducing, whereas the capacity peak values  $B\eta_T$  fall at same value  $B$  – just as it follows from the theory of similarity of energy conversion processes. Thus the non-linearity of the processes running in the vortex tube tells on mostly the locations of the said peak values. In particular, the location of the capacity peak changes from  $B = 0.5$  to  $B =$

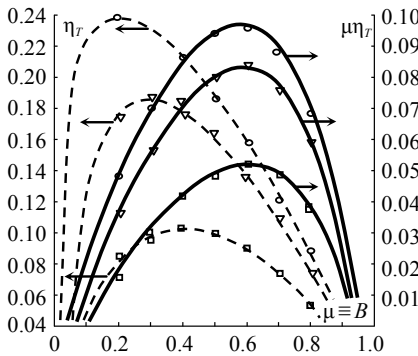


Fig.18.5. Load Characteristics of vortex-type gas energy separators

0.55...0.6. This allows using the deductions of thermokinetics for analysis of real machines thus facilitating the choice of their optimal operating conditions.

The fact the max efficiency and max power operating conditions exist is also confirmed by the efficiency curves of electro-technical energy converters, characteristics of pumps and fans, velocity characteristics of internal combustion engines, etc. All this evidences that thermokinetics correctly mirrors the general

mechanisms of non-static energy conversion processes thus moving one step further toward the reality.

The demonstration of unity between the energy conversion processes in thermal and nonthermal engines would be more com-

plete if, along with the technical devices above considered, the operation of the muscular mover as an example of a biochemical energy converter is also analysed.

Let us consider for example the fibril as a muscle element converting chemical energy into mechanical one. In this case the generalized rate  $\mathbf{J}_i$  of the primary process is construed as the flow  $\mathbf{J}_r$  of the substances taking part in this chemical reaction, while the generalized rate  $\mathbf{J}_j$  of the related process – as the muscle traction rate. Each of these flows according to (16.6.3)–(16.6.4) depends on both forces, the first of which,  $\mathbf{X}_i$ , is now construed as the negative gradient  $-\text{grad}(A_r\lambda_r)$  of chemical reaction affinity, while the other – the fibril contraction  $\mathbf{X}_j$ . Note that when the chemical reaction runs thru to the end ( $\xi_r = 1$ ), the force  $\mathbf{X}_i$  is equal to the chemical reaction affinity  $A_r$ .

Laws (16.6.3) and (16.6.4) may be more conveniently represented in dimensionless form not containing phenomenological coefficients. To do so, let us consider the so-called “isometric muscle traction” condition (analog of the engine/welding transformer no-load operation). At this condition the force  $\mathbf{X}_j$  reaches its peak value  $\mathbf{X}_{j_0}$  (no-load strength) when  $\mathbf{J}_j = 0$ . This condition is opposed by the so-called “unloaded muscle traction” condition (analog of the transformer secondary winding short circuit) when  $\mathbf{X}_j = 0$ , while  $\mathbf{J}_j$  is equal to the short-circuit current  $\mathbf{J}_{jk}$ . Expressing  $\mathbf{X}_{j_0}$  and  $\mathbf{J}_{jk}$  according to (16.6.3) and (16.6.4) in terms of the phenomenological coefficients gives at  $\mathbf{X}_i$  being constant:

$$X_j/X_{j_0} + J_j/J_{jk} = 1. \quad (18.6.11)$$

Such a form of the phenomenological laws still more stresses the unity of energy conversions in any forms. In a more general case of the phenomenological coefficients as some power functions of the relating forces  $L_{ii} = L_{ii}(X_j/X_{j_0})^a$  и  $L_{jj} = L_{jj}(J_j/J_{jk})^a$ , where  $a$  is an experimental value, these equations become non-linear:

$$(X_j/X_{j_0})^{1+a} = (1 - J_j/J_{jk})^{1+a}. \quad (18.6.12)$$

The character of such semi-empirical laws with a various value of the exponent  $(1+a)$  equal to 1.0, 1.15, 1.3 and 1.5 is plotted on Fig.18.6 in the form of curves 1, 2, 3 and 4, respectively. As follows from the figure, at  $a = 0$ , the relationship  $X_j/X_{j_0}$  vs.  $J_j/J_{jk}$  is linear (straight line 1). The higher the exponent “ $a$ ” is, i.e. the stronger the dependence of phenomenological coefficients on forces is, the more non-linear the curve becomes. However, this non-linearity is caused by exclusively the non-linearity of laws (18.6.3)–(18.6.4) proper and has nothing to do with relating the rates of both processes, i.e. the flows  $J_j$  and  $J_j$  as sometimes imag-

ined (Keplén, Essig, 1968). Let us, for comparison, consider the Hill's empirical equation which accurately enough characterizes the muscles for different kinds of animals:

$$(X_j/X_{j_0} + \alpha_0)(J_j/J_{jk} + \alpha_0) = (1 - \alpha_0)\alpha_0, \quad (18.6.13)$$

where  $\alpha_0$  is a value Hill named the "efficiency index" for muscle. It is connected with the value  $q_x = L_{ii}/(L_{ii}L_{jj})^{0.5}$  he named the "flow relation factor" by the relationship  $q_x = 1/(1 + \alpha_0)^{0.5}$ , i.e. is a function of the quality factor  $\alpha_0 = \Phi - 1$  we earlier introduced. The Hill's curves for various  $q_x$  well correspond to those plotted on Fig.18.6, i.e. the higher the flow relation factor  $q_x$  is, the more non-linear the curve becomes. At the same time the curves of (18.6.13) basically differ from the Hill's curves in the interpretation of what causes the non-linearity of the phenomenological

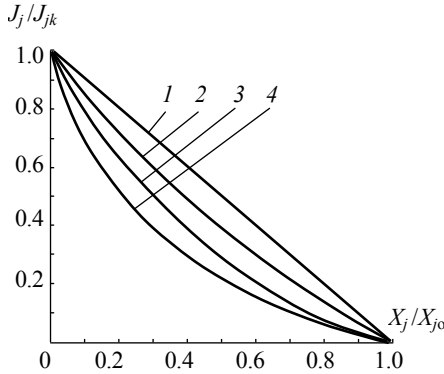


Рис. 18.6. Load Characteristics of muscle element

laws. By Hill the linear relationship  $X_j/X_{j_0}$  vs.  $J_j/J_{jk}$  corresponds to the value  $L_{ii}/(L_{ii}L_{jj})^{0.5} = 0$  (or  $\Phi = \infty$ ), i.e. to the trivial case of  $L_{ii} = -L_{jj} = 0$ . However, the fact the relation factor becomes zero means no interrelation between the flows  $J_i$  and  $J_j$ , i.e. no energy conversion itself! So the non-linearity of phenomenological laws has appeared to be connected with the muscle movers' efficiency.

It is worth generally noting that this absurdity is far from being the only one when the investigation of chemical-to-mechanical energy muscular converters is provided by the TIP methods formally transferred to biosystems (S. Keplén, E. Essig, 1968; A. Rubin, 1984; et al.). In this connection the kinetic equations of metabolism and energy conversion processes in muscular movers are expressed in the form of Onsager's linear phenomenological laws (5.1.6) wherein the flows  $J_i$  and forces  $X_j$  are derived from the expression for the entropy generation rate (see 5.1.4). This looks quite logic until the investigator encounters the efficiency ambiguity for such converters showing in the fact that according to (5.1.4) the entropy generation may be resolved into the components  $J_i X_i$  and  $J_j X_j$  voluntarily (S. De Groot, R. Mazur, 1964). In fact, the only TIP requirement when choosing flows and forces is that the total entropy generation be maintained (invariance of dissipation func-

tion (5.3.3) characterizing the dissipation power). Doubts in the TIP applicability grow even stronger when the different-kind forces  $X_i$  and  $X_j$  relate to the same (even or odd) time functions. In this case the Onsager's (but not Casimir's) symmetry conditions must be observed, for which the requirement the matrix of phenomenological coefficients to be positively defined is expressed as the restriction  $(R_{ij} + R_{ji})^2 < 4R_{ii}R_{jj}$ . In this case  $\Phi \leq 1$ , and the efficiency of any energy converters can not be in excess of about 17.5% (which does not naturally occur in reality). The point is that in the energy conversion processes, unlike the transfer processes, the dissimilar fluxes  $J_i$  and  $J_j$  are interrelated. Therefore the reciprocal relations of energy conversion processes bear invariably asymmetrical character, while their phenomenological laws have the form of (18.4.1), (18.4.2). For such laws the above limitations on the Q-factor value are invalid.

This fact once again confirms the inadmissibility of TIP formal transfer to the energy useful conversion processes (V. Etkin, 1995). On the other hand, we have a one more confirmation of the fact that ergodynamics correctly describes the general laws of nonstatic energy conversion processes and makes in this respect one more step toward reality.

## *Chapter 19*

### **THEORY OF ENGINEERING SYSTEMS PRODUCTIVITY**

Perceiving the rate and the productivity of real processes as one of their efficiency criteria has revealed two more branches in thermodynamics of the XX<sup>th</sup> century along with the theory of irreversible processes (TIP) and called, respectively, "thermo-economics" and "finite-time thermodynamics" (FTT). Of the two branches, the former originates in the M. Tribus's and his research fellows' works (Tribus, Evans, Crellin, 1966) and is intended for commensuration of savings in current fuel and materials due to machine efficiency upgrade with the investments associated. Introducing economics elements in thermodynamics modifies the engineering system efficiency criteria themselves since not the maximum of efficiency optimizes now the parameters of engineering systems, but the minimum of their planned costs. This direction involving also the heat exchange theory along with thermodynamics was further developed and widely applied in our country largely due to the works by A. Andrushchenko and his school (1974).

The second branch assigned a top priority to define conditions to obtain maximal economic efficiency considering restricted contact of working medium in power plants with heat well and heat sink. This is the theory that first and most generally framed the question of interrelation between power (productivity) of engineering systems and their thermodynamic efficiency, i.e. of essentially the extreme capabilities of real processes given their irreversibility. However, this theory in the available form is suitable for only the machines operating under maximum power conditions. In this context quite topical is the question how to construct a more general theory of engineering systems productivity, which should comprise both of the said branches as particular cases and relate to the classic theory of heat engines the same way as dynamics to statics.

### 19.1. Synthesis of Thermokinetics with Thermoeconomics

The abovementioned independent development of the three branches of present-day thermodynamics (theory of irreversible processes (TIP), thermo-economics and finite-time thermodynamics (FTT)) is largely conditioned by the difference in efficiency criteria for the real (non-static) energy transfer and conversion processes these branches investigate. These criteria are as follows: for TIP – minimum of entropy generation in a system  $\sigma_s$  (De Groot, Mazur, 1964); for thermo-economics – minimum of machine planned costs  $3_p = \min$  (A. Andrushchenko, 1963; M. Tribus, 1970); for FTT – maximum of machine output power  $N_j = \max$  (Barrer, 1982; Rudenko, Orlov, 1984). Creation of thermokinetics as a unitary thermodynamic theory of real processes and the associated theory of similarity of power and processing plants allows including load and productivity of such machines in the number of the parameters being optimized. This facilitates elaborating a unitary efficiency criterion for power and processing plants and creating on its basis a theory of engineering systems productivity considering not only thermodynamic parameters, but also operation condition and cost.

Let us adopt for an objective function when optimizing the operation conditions of operating power and processing plants the maximal benefit  $\Pi$  defined as the difference between the sales income (VAT and excise tax not included) and the production and sales expenses as included in the production cost. Dividing, as usual, the production expenses into the variable depending on production output  $\mathcal{E}$  and the conditionally constant  $\mathcal{C}$  and relating the variable expenses to the production output the objective function may be represented as:

$$\Pi = (\hat{g} - \alpha)\Theta - C = \max, \quad (19.1.1)$$

where  $\hat{g}$  means the finished product unit price, while  $\alpha$  – variable component of unit cost.

Let us consider this expression together with the generalized relationships between power and productivity of machines offered by the theory of their similarity. Let us consider, in  $N$  – machine mean power,  $\tau$  – machine operating hours;  $\hat{g}$  – power release price, \$/kWh;  $\hat{g}^*$  – value close to fuel cost component in total power cost, \$/kWh). Representing the fuel cost component  $\hat{g}^*$  as the product of the fuel price  $p_f$  (\$/kg) by the fuel rate  $b_f$  (kg/kWh) and expressing the latter in terms of its minimal (theoretical) value  $b_f^0$  (corresponding to  $\eta_N = 1$ ) as  $b_f = b_f^0/\eta_N$  the objective function may become:

$$\Pi = (\hat{g} - b_f p_f) N \tau - C = \max. \quad (19.1.2)$$

Let us now express this objective function in terms of the machine load  $B$  using the generalized relationships relating the machine power and efficiency  $\eta_N$  with load criterion (18.4.8):

$$\Pi = [(\hat{g} - b_f p_f)(1 + 1/B\Phi)/(1 - B)] N_{\max} B(1 - B) - C. \quad (19.1.3)$$

Maximizing this expression as the load function  $B$  by equating its derivative to zero gives after some transformations:

$$B_{\text{opt}} = 0,5(1 - \eta_N \alpha). \quad (19.1.4)$$

where  $\alpha = b_f p_f / \hat{g}$  – fuel component share in the total electric power price.

Substituting (19.1.4) into (18.5.4) gives an expression for the machine power economically most advantageous:

$$N_{\text{opt}}/N_{\max} = 1 - (\eta_N \alpha)^2 \quad (19.1.5)$$

According to this expression, the less the fuel component of power price (and more generally – variable costs component in product price) is and the less economical the machine is, the closer the nominal power approaches its peak value. The relationships (19.1.4) and (19.1.5) are more demonstrably plotted on Fig. 19.1. The complex  $\eta_N \alpha$  values varying from zero to unit are plotted here on the abscissa, while the machine relative loads and powers economically most advantageous are plotted on the ordinate. As follows from the figure, with  $\alpha \rightarrow 0$  or  $\eta_N \rightarrow 0$  the optimal load  $N_{\text{opt}} \rightarrow N_{\max}$ . This result is characteristic for machines

on renewable energy sources (hydropower stations, tidal, wave, wind, solar and geothermal power stations) and complies with the efficiency criteria of finite-time thermodynamics.

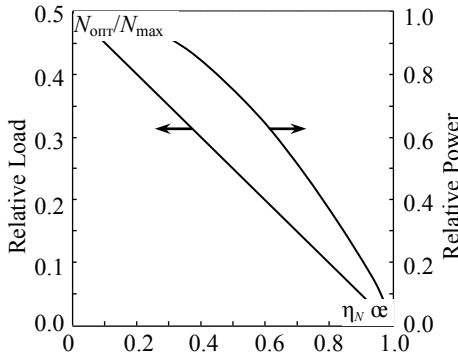


Fig. 19.1. Operating Conditions Economically Most Advantageous for Power Plants

On the contrary, with cost factors neglected ( $c_T \approx 0$ ) quasi-static processes ( $B \approx 0$ ) appear to be most advantageous. This result complies with the thermodynamic approach where the machine efficiency is the only criterion. Machines with a considerable variable costs share occupy an intermediate position. E.g., for thermal power stations with a power efficiency of  $\eta_N \approx 0.45$  and a fuel component in product price of  $\alpha \approx 0.6$  the optimal load

$B_{opt}$  is equal to 0.36 and close to the nominal one corresponding to the utmost economic efficiency of a machine with the  $\Phi$ -factor  $\Phi \approx 4.5$  (Fig. 18.2). This result complies with the efficiency criterion of thermokinetics since for a machine with a specified productivity (operating to a specified load curve) the peak of benefit corresponds to operating conditions with minimal specific fuel rates  $b_T = \min$ . Thereby thermokinetics as if “lays a bridge” between classic thermodynamics, thermo-economics and finite-time thermodynamics and allows to put further questions of optimal operating conditions definition for power and processing plants of various types.

## 19.2. Nominal Operating Conditions for Power Units

Including load in the number of factors to be optimized enabled determination that maximum of efficiency for power and processing plants of various kinds was far from being always corresponding to their peak power. In particular, for a big group of thermal power plants operating to a specified load curve  $B_{opt}$  corresponds to nominal operating conditions (with minimal fuel rate). This demands the loads to be optimally distributed between the power units of a thermal power station. The solution to this rather laborious problem is considerably facilitated due to the available universal load curves for energy converting systems and due to the possibility to plot on their basis individual load curves for various types of power units despite a restricted scope of information. To do this, the data of full-scale test on all power units or aggregates should be presently



available. To obtain such data, considerable time and costs are needed; therefore such tests are extremely seldom with the results often becoming obsolete yet in the period between overhauls. Besides, the calculations of fuel rate increment per unit power increase for any operating conditions of a machine the existing methods of load distribution are based on are so complicated and laborious that their application is far from being always paid back. Therefore in practice a known principle has to be followed, which reads that more economical machines should be loaded first of all. Nevertheless, this statement is far from being always true. Let us assume there are two power units on a thermal power station with the same installed power and good quality factors  $\Phi = 4.7$  and  $3.0$ . Then according to criterion equation (18.4.8) the relative load of the first power unit being increased from  $0.2$  to  $0.3$  will increase its power efficiency  $\eta_N$  from  $0.387$  to  $0.409$ , i.e. by  $0.022$ , whereas for the less economical unit with  $\Phi = 3.0$  this efficiency will increase from  $0.30$  to  $0.331$ , i.e. by  $0.031$ . Hence, the second power unit being loaded will provide a higher both absolute and relative increase in economic efficiency of the entire thermal power station and a lower increase in its fuel rate. In other words, everything depends on the working point position on the universal load curves of a machine. Fig. 18.2 visually demonstrates this statement. E.g., the load of a machine operating with maximal  $\eta_N$  being increased, its economic efficiency may even decrease, whereas the same for another machine operating under loads considerably inferior to nominal will cause steep increase of its economic efficiency. In this context the visualization of operation conditions for power system units in the form of an array of working points on the universal curve of the Fig.18.2 type facilitates the solution to the problem posed since allows, subject to reasonable accuracy of the prognostic estimates, cutting the expenses to conduct relevant tests and calculations.

To illustrate plotting and using individual load curves, let us consider an arbitrary condensing steam turbine plant. The individual load curve for such a machine can be plotted in linear approximation as based on the information about its operation at one of the operating conditions with subsequent reconstruction of the efficiency and power curves configuration on the basis of criterion relationships or universal curves. A working point may be found on Fig.18.2 by several ways. Firstly, this may be done based on the records of the power unit mean load for some time period and of equivalent fuel consumptions for the same period, which allows calculating the equivalent fuel rates  $b_r$  followed by determining the machine exergic efficiency  $\eta_N = 3600/b_r p_f$  in terms of the exergy  $e_r$  known. The relative load  $B$  can be herein found according to (19.1.4) as the ratio of generator currents at the present / short circuit operating conditions. E.g., for the T $\Phi$ -series 63MW generators the rated current and short-

circuit current are 7,210A and 24,000A, respectively, i.e. their relative load at nominal conditions is 0.3. Ultimately, a working point can be also found by known quality factor  $\Phi$  of the steam turbine plant, which can be estimated as based on its recorded cycle parameters. Let the steam turbine plant be operating, for example, at mean thermodynamic temperatures of the heat well (fuel combustion products) and heat sink (circulating water) equal to  $T_h = 1,120\text{K}$  and  $T_c = 295\text{K}$ . If the mean thermodynamic temperatures of heat application and heat abstraction in cycle are in this case  $T_1 = 625\text{K}$  and  $T_2 = 305\text{K}$ , respectively, while the effective efficiency of the steam turbines  $\eta_{oe} = 0.87$ , then neglecting the feed-water pumps operation the quality factor of the entire steam turbine plant may be assessed in linear approximation by replacing the resistance relationship by the relationship between the adequate integral forces. As a result of calculation the quality factor for the steam turbine plant under consideration can be found according to (18.3.6) as  $\Phi = 4.57$ . For this value the load economically most advantageous is according to (19.5.1)  $B_n = 0.297$ , while the peak value of the power efficiency  $\eta_N = 0.40$ . Thus rather simple calculations allow assessing the quality factor of an operating power plant and plotting, as based on the quality factor, (in linear approximation) the total load curve of this power plant without additional experiments. In that way the similarity theory-based express methods channel the load optimal distribution issue in the practical direction.

### 19.3. Optimal Overload Degree of Power and Processing Plants

We have considered above the case when the peak of economic efficiency of power and processing plants was associated with their operation under the relative loads either maximal or close to such. However, according to Fig. 15.2, there is a rather wide spectrum of operating conditions in-between those of maximal power and maximal economic efficiency usually taken as nominal, which may be called overloading or boosting. Such operating conditions are quite characteristic for overland, air and space vehicles. They occur in also stationary power plants intended for irregular load curve operation. However, the choice of power augmentation optimum has not been hitherto considered with due regard. In power engineering this is explained so that the nominal operating conditions of power units are close to their limit power (according to the technical operation standards an electric generator may be overloaded for several seconds to several minutes); in other cases the interest in the problem is restricted because power units operate according to an assigned load curve or because the thermodynamic mathematical tool can not be

applied to their analysis in finite-time format. It can only add to the interest to consider these issues from the thermokinetic positions.

According to expression (16.1.4) the economically most advantageous load  $B^{opt}$  at the utmost high fuel cost component  $\alpha = 1$  is defined by exclusively the efficiency of a machine and corresponds to minimal fuel rate.

Such loads are usually taken for the nominal  $B_n$ . For them the ratio  $B^{opt}/B_n$  is evidently equal to unit. With  $\alpha$  decreasing at  $\Phi = \text{const}$  (and, hence, at  $B_n$  and  $\eta_{ex}$  being invariable in the nominal operation) the optimal loads increase, and the machine operation becomes economically justified for loads exceeding those nominal, i.e. in the so-called augmentation operation.

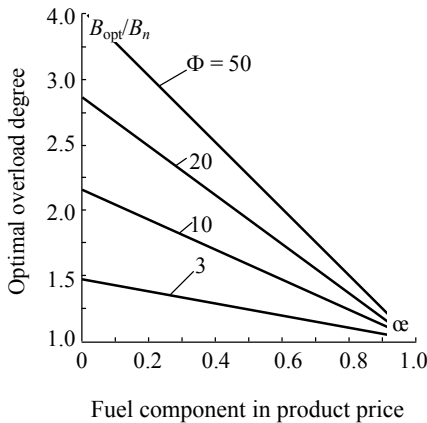


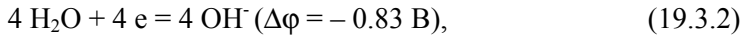
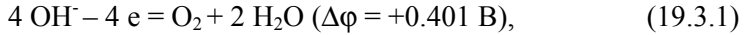
Fig.19.2. Optimal Overload Degree for Power Plants

The economically most advantageous augmentation level evaluated by the  $B^{opt}/B_n$  ratio can be found from (19.1.4) and, for a higher degree of generality, expressed as a function of the quality factor  $\Phi$ . Such a relationship is illustrated on Fig.16.2. According to the generalized graphs plotted therein the economically justified overload degree for power and processing plants increases with their quality factor.

If, e.g., for steam turbine plants with the quality factor  $\Phi = 3...4$  at the fuel cost component in the total power price  $\alpha \approx 0.5$  the economically most advantageous overload degree is 1.25...1.35 (which means the power overload by only 4.1% at  $\eta_N \approx 0.4$  and according to (16.1.4), then the problem of using overload operations is well actual for highly economical processing plants.

Let us consider, for a specific example, an electrolysis plant to extract hydrogen and oxygen from water, which exergy analysis is described by Nesterov in his work (1980). The plant consists of an electrolysis cells battery, gas-liquid solution separation units, electrolysis gas purification and dehydration units, heatexchangers and pumps. The power supply to the plant includes the electric power  $N_{el}$  and the flows of commercially suitable energy (exergy) with initial reagents  $Ex_p$ . The plant productivity in whole is defined by the amount of the hydrogen and oxygen produced. Its energy (exergy) equivalent is construed as the power  $N_j$  defined by the flows of commercially suitable energy of electrolysis products  $Ex_{pr}$  and heat carriers  $Ex_h$ . In the scheme under consideration wa-

ter is fed to the plant from outside, while gases are removed from the battery together with electrolyte. The plant power  $N_j = 1,500$  W, battery voltage 1.95 V. The ambient air temperature and pressure are  $T_0 = 298$  K,  $p_0 = 0.1013$  MPa, respectively. To represent the operational conditions of such a plant in terms of the similarity theory, let us consider the electrochemical reactions running in the anode and cathode parts of the electrolysis elements:



where  $\Delta\phi$  – potential difference across the proper electrode,  $e$  – designation of electron as a system component.

As follows from (19.3.1) and (19.3.2), EMF of this reaction is equal to 1.23V, which corresponds to a battery power efficiency of  $\eta_N = 0.63$  (a more detailed calculation gives  $\eta_N = 0.621$ ). In this case the voltage drop across the battery internal resistance is 0.72 V, which corresponds to the relative load  $B = 0.72/1.95 = 0.37$ . According to the universal load curves such parameters refer to a plant with the quality factor  $\Phi \approx 50$ . The optimal overload degree for this plant according to Fig.19.2 is 2.5...2.25 at  $\alpha \approx 0.4 \div 0.5$ . As a matter of fact, the plant operates with even higher overload. Indeed, for a plant with  $\Phi \approx 50$  according to the universal curves on Fig.13-2 the nominal operating conditions are associated with the relative load  $B \approx 0.12$  and  $\eta_N = 0.77$ . Thus the plant under consideration actually operates under a threefold overload relative to the most economically advantageous operating conditions, which is economically justified subject to a moderate price for electric power ( $\alpha \approx 0.2$ ). Hence, this plant has some reserves in economic efficiency upgrade. Anyway, this example tells it is expedient to modify the operating conditions of processing plants according to market-determined prices for finish products and electric power. This fact taken into consideration at market economy may become an extra incentive to maintain optimal operating conditions of equipment and to update the existing power and processing plants in order to extend their overload capabilities under the finished product deficiency.

#### 19.4. “Cruising Speed” Operation of Transport Vehicles

For transport vehicles of a wide spectrum the peak efficiency as per condition (16.1.4) does not correspond any more to the peak power of their propulsion systems. The point is that the power augmentation en-

tails increasing the fuel rate and the fuel load required to deliver a cargo in self-sufficient sea or air freight, which results in the adequate reduction of the net load being carried, i.e. in the drop of the vehicle capacity. The reduction in income from vehicle running thus caused can be accounted for in (19.1.2) by adequately increasing the costs for transportation of fuel itself. In this case in (19.1.2) along with the term  $b_{\tau}b_f$  characterizing the fuel component in the variable costs an additional cost summand will appear proportional to the transportation power inputs with a proportionality factor equal to the unit fuel transportation cost  $b_{tr}$ :

$$\Pi = [\hat{g} - b_{\tau}(b_f + b_{tr})]N\tau - C = \max . \quad (19.4.1)$$

Due to this the optimal load on the vehicles' propulsion systems defined by expression (19.1.4) will decrease a little as compared with the peak power operating conditions and will be now associated with the cruising speed of a ship or aircraft corresponding to the minimal fuel rate and, hence, to the minimal mass of the vehicle itself. Minimum mass of a transport vehicle at the given power of its propulsion system will evidently provide the transportation of the maximal cargo, i.e. corresponds to the maximal capacity of the vehicle. Therefore, the problem of transport vehicle mass minimization is one of the most important design and operational targets. This issue is of utmost importance for space vehicles where the net mass of the cargo being transported often defines the range and duration ability of the vehicle, i.e. the feasibility of particular space programs.

Let us consider for example the total mass minimization problem for a space vehicle proceeding from the only requirement to deliver a specified net cargo while moving in a specified path (Etkin, 1996). Such an approach assumes the definition of the so-called characteristic velocity of the space vehicle  $v$  as the sum of its velocity increment magnitudes  $\Delta v_i$  at particular stretches of its path. For space vehicles starting off from the satellite orbit this velocity is usually counted off from the orbital velocity and defined by the Tsiolkovsky's formula:

$$v = w \ln(M_k/M_o) , \quad (19.4.2)$$

where  $M_k$ ,  $M_o$  – initial and final mass of the flying vehicle (with propulsions on and off), respectively;  $w$  – jet stream velocity assumed constant.

Since  $M_o = M_{\Delta} + M_{\Pi} = M_k - M_{\tau}$ , relationship (16.4.2) gives:

$$M_{\tau} = (M_{\Delta} + M_{\Pi})[\exp(v/w) - 1] . \quad (19.4.3)$$

Then the total mass of the space vehicle is equal to:

$$M_k = (M_d + M_n) \exp(v/w) . \quad (19.4.4)$$

Now let us express  $M_d$  in terms of the specific (related to the jet stream kinetic energy) mass of the propulsion system  $\gamma_d = 2M_d/Gw_c^2$ . Then:

$$M_k = (\gamma_d G w_c^2 / 2) \exp(v/w) + M_n \exp(v/w) . \quad (19.4.5)$$

Equating the derivative of this expression with respect to the velocity  $w$  to zero under the assumption of  $v$ ,  $G$ ,  $\gamma_d$  and  $M_n$  being constant gives:

$$2w - v - M_n v / w^2 G \gamma_d = 0 . \quad (19.4.6)$$

Introducing for convenience the net cargo share  $\rho_n = M_n / M_d^{\text{opt}}$  as the ratio of the cargo mass  $M_n$  to the optimal mass of the propulsion system (at  $w = w_{\text{opt}}$ ) and considering that  $2M_n v / G \gamma_d w_{\text{opt}}^2 = \rho_n v$  gives finally:

$$(w/v)_{\text{opt}} = (1 + \rho_n) / 2 \text{ или } R_{y_d}^{\text{opt}} = (1 + \rho_n) v / 2g, \quad (19.4.7)$$

where  $R_{\text{sp}} = w/g$  – the so-called specific jet thrust ( $g$  – gravitational acceleration).

According to this equation the optimal specific thrust value  $R_{\text{sp}}^{\text{opt}}$  at  $v$ ,

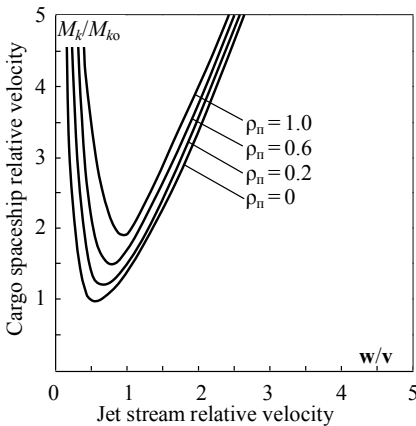


Fig.19.3. Spacecraft Specific Thrust and Net Cargo Optimization

$G$ ,  $\gamma_d$  and  $M_n = \text{const}$  does not depend on the flight duration, propulsion system efficiency and specific gravity and is defined by exclusively the flight path ( $v$  value) and the cargo net weight. That resulted from a more general problem definition, which did not assume the constancy of the propulsion system power  $N$ , full thrust  $R$  and the specified flight duration  $\tau$  and demanded a minimal scope of initial data. The solution to the problem in the form of (19.4.1) and (19.4.2) has the same general character and is valid regardless the type of the jet engine,

its design and size features. At the same time such an approach to choosing  $R_{\text{sp}}^{\text{opt}}$  leaves enough freedom to choose the propulsion system power  $N_p = Gw^2/2$ , working medium consumption  $G$  and propulsion full thrust  $R$ ,

and, hence, the active propulsion time  $\tau$ . It is significant that the value  $R_{sp}^{opt}$  defined by (16.4.2) is considerably lower than that found under constancy of the jet propulsion full thrust  $R$  and the specified active flight duration  $\tau$  and considerably closer to the optimal relationship between the jet outflow and flight velocities  $(w/v)_{opt}$ , which is equal to unit and corresponds to the peak value of the jet engine power efficiency.

Fig.19.3 illustrates the relationship according to expression (16.4.5) between the spacecraft mass  $M_k$ , net cargo mass  $M_n$  and the velocity ratio  $w/v$ . For a better generality the values  $M_k$  and  $M_n$  are related therein to the spacecraft optimal mass  $M_{k0}$  calculated from equation (16.4.5) in the absence of the net cargo and, thus, with the optimal ratio  $(w/v)_{opt} = 1/2$ . As follows from the figure, the minimal ratio  $M_k/M_{k0}$  (optimal  $R_{sp} = w/g$ ) with the net cargo share increasing shifts, as should be expected, toward higher values of the outflow velocity. However, the deviation from the optimal ratio  $w/v$  results, at the conditions accepted, to a steeper increase of the  $M_k/M_{k0}$  value than at the constant thrust of propulsions. The spacecraft mass increases especially sharply with the  $w/v$  ratio reaching some minimal value, which evidences that the application of engines with a specific thrust below the said value is unpractical. E.g., for the “round trip” flights to Venus or Mars (when the minimal characteristic velocity is equal to 3.7-3.8 km/c (Yavorsky and others, 1970)) with the net cargo mass  $M_n = M_n^{opt}$  the application of a liquid-propellant rocket engine on components of the “oxygen-gasoline” or “nitric acid-kerosene” types (with a specific thrust of 260-300hp) is practically excluded. Engines of other types have to be used for these purposes, in particular, the nuclear-fission rockets with specific thrusts of 750-800hp on hydrogen operation. The more general relationships obtained here between the spacecraft mass and velocity parameters may be useful for also determining the ranges of required specific and full thrusts, propulsion system type and power, as well as a number of other parameters of a space rocket engine for particular space flights.

## 19.5. Peak Power Reach Conditions for Heat Power Plant

Classic thermodynamics is known to have posed and solved the problem of determining the most economical thermodynamic cycles (with maximal thermal efficiency or heat transformation ratio) within a specified temperature range. These are known to be the ideal Carnot cycles. Classic thermodynamics characterizes with a conclusion that the maximal efficiency of heat engines does not depend on the properties of the working medium (its state equations) and is defined by solely the temperature interval within which the cycle is realized. However, the duration of real

thermodynamic processes is finite, while their efficiency depends on not only the perfection degree of the heat-into-work conversion, but on also the intensity of the heat exchange between the working medium and the heat wells. Therefore the real cycle efficiency is always overestimated. This fact poses the problem of revealing the limiting capabilities of real processes considering not only the temperatures of heat wells, but also the heat transfer coefficients, duration of a cycle in whole and its particular stages, cycle-averaged power, etc. Curson and Ahlborn were the first who proposed such a problem definition (1975) having considered the conditions of developing a Carnot cycle providing the peak cycle-averaged power  $N$  at temperatures of heat well and heat sink of  $T_h$  and  $T_c$ , respectively. In this definition the working medium receives and releases heat at the constant temperatures  $T_1 < T_h$  and  $T_2 > T_c$ . (Curson, Ahlborn, 1975). The optimal values of these temperatures are to be found here corresponding to the cycle peak power at a contact duration between the working medium and the heat well and heat sink of  $t_h$  and  $t_c$ , respectively, when the heat flows in-between them obey a linear law of the type:

$$J_q' = L_h(T_h - T_1) ; \quad J_q'' = L_c(T_2 - T_c) , \quad (19.5.1)$$

where  $L_h, L_c$  – constant heat transfer coefficients.

Settling the values of the parameters  $t_h$  and  $t_c$  as satisfying the limitations  $J_q'/T_1 + J_q''/T_2 = 0$  (ensuing from the entropy variation cyclic character) the authors express the power  $N = (J_q''t_h + J_q't_c)/t$  averaged thru the cycle duration  $t_h + t_c = t$  as a function of above parameters and find the peak of this function allowing for the said limitations. In this case the thermal efficiency corresponding to the cycle peak power  $N_{\max}$  is defined by the relation:

$$\eta_t^{opt} = 1 - \sqrt{T_c / T_h} . \quad (19.5.2)$$

As can be seen, the optimal thermal efficiency of such a cycle is considerably lower than the ideal Carnot cycle efficiency at the specified values  $L_h, L_c$  of heat transfer coefficients and the peak power.

Many works dedicated to thermodynamics of finite-time processes are characteristic by the fact that they consider limitations of various kinds, viz. for working medium minimal and maximal volumes (Curson, 1975; Rubin, 1980), for piston acceleration in internal combustion engine (Band, Kafry, 1981), for heat amount  $Q_h$  received from a heat well (Rubin, 1979; Band, 1982), etc. A great number of works in this field are dedicated to investigation of systems where the heat flow from a heat well to the working medium is considered as given in the form of some time



function  $J_q(t)$  (Salamon, 1981; Fairen, 1982). It is worth noticing that the first overview of works dedicated to finite-time processes thermodynamics (Barrer, 1982) was published in France as early as in 1980. It is mentioned therein that taking the time factor into consideration when optimizing the cycles of heat engines allows estimating the efficiency of real plants relating their parameters to the limiting parameters of irreversible cycles having the same power, heat transfer coefficients, duration, etc. Thus the finite-time thermodynamics reveals the limiting capabilities of energy conversion irreversible processes in heat engines at finite duration of the heat application and abstraction processes (and, consequently, finite duration of the cycle), as well as under various limitations to the plant parameters. Its methods are starting to be successfully applied to estimate the efficiency of not heat engines only, but also processing plants, in particular, the photovoltaic cell-based plants and the plants of water decomposition into oxygen and hydrogen (Dung, 1982). Attempts are known to optimize by this method the chemical efficiency of tubular reactor (Ondrechem, 1980), as well as the output power of pulsating laser (Keren, 1982) and the installation using the radiant energy (Adler, 1981; Mozurkewich, 1983). Thus the application sphere of finite-time thermodynamics is rapidly widening (Linden, 1992). This is promoted by not only the need to clarify the limiting capabilities of thermodynamic processes. Posing the problem in this theory changes the efficiency criteria for heat engines and processing plants bringing them closer to reality. At the same time it is worth noticing that finite-time thermodynamics considers only the so-called externally irreversible cycles where the cycle-comprising processes themselves are considered equilibrium (internally reversible). Such inconsequence is explained by the fact that finite-time thermodynamics imports the transfer equations involving the process rate from outside, i.e. from the heat exchange theory. Process time and productivity do not now, as before, enter in the equations of finite-time thermodynamics which is thus incapable to describe the kinetics of the thermodynamic systems' transfer from some non-equilibrium state into another (i.e. the motion of such systems). Furthermore, this theory is based on solely the cycle method and is therefore inapplicable to the analysis of the heat energy direct conversion plants, as well as to the flow-type machines. Besides, it does not consider the kinetics of energy-conversion process itself and assumes that the duration of arbitrary cycle in finite-time thermodynamics is added of only the times of heat application and abstraction. In the absence of unanimous approaches to the energy dissipation in the energy transfer and conversion processes the circle of problems solvable by the methods of finite-time thermodynamics appears to be considerably limited. In this respect the synthesis of thermodynamics and economics – “thermoconomics” – offers a noticeable advantage.

This direction in thermodynamics of the XX<sup>th</sup> century is aimed to commensuration of savings in fuel and material due to plant efficiency upgrade and the investments associated. At the same time it should be noted that the irreversibility of useful work processes in thermo-economics is also considered not on the basis of their kinetics study, but by introducing constant relative efficiencies of these processes, i.e. without the relationship between power and cost effectiveness of engineering systems taken into consideration. From here the problem ensues to directly introduce the factor of real process productivity (useful power) into the equations of thermodynamics as a thermodynamic variable along with the process time and rate. This problem has been solved in thermokinetics that does not exclude from the consideration the irreversible part of a real phenomenon (like in Thomson's pseudo-thermodynamics) or its reversible part (like in Onsager's quasi-thermodynamics) and may be applied to investigation of processes with any degree of irreversibility.

As shown above, in search of conditions to reach the peak cycle power finite-time thermodynamics proceeds from the ideas usual for thermodynamics about the possibility to vary the durations of heat application  $\Delta t_1$  and abstraction  $\Delta t_2$  processes in cycles and to include them in the number of the parameters being optimized (Curson, Ahlborn, 1975). In this case the optimal duration of contact between the working medium and the heat well and sink appears to be dependent on the heat transfer coefficients. However, these ideas appear to be invalid when considering a steady-state energy conversion process in a thermal power plant. As shown above, the availability of a "transit" (crossing the system invariable) flow of corresponding energy carrier is the necessary condition of useful work done. For heat engines this is expressed as the equality of total entropy flows entering and leaving the engine  $J_s' = -J_s''$  (16.2.7). Comparing this condition with (16.2.6) and taking into consideration that for any cycle  $\Delta S_1 = -\Delta S_2$  drives to a conclusion that the durations the working medium contacts with the heat well and heat sink are equal to each other:

$$\Delta t_1 = \Delta S_1 / J_s' = \Delta S_2 / J_s'' = \Delta t_2 . \quad (19.5.3)$$

Thus, unlike finite-time thermodynamics, thermokinetics introduces the additional condition  $\Delta t_1 = \Delta t_2$ . This provides such a result that the temperatures of heat application  $T_1$  and abstraction  $T_2$  appear to be interrelated. To reveal this relationship, let us consider the identity of the mean thermodynamic heat application and abstraction temperatures  $T_1$  and  $T_2$  to the mean integral temperatures of the heat flow entering and leaving the plant  $T'$  and  $T''$ , which is ascertained in the previous chapter. This allows

expressing the thermal efficiency of an arbitrary cycle in terms of the heat flow parameters:

$$\eta_t = 1 - \bar{T}_2/\bar{T}_1 = 1 - T''/T' = 1 - J_q''/J_q'. \quad (19.5.4)$$

Representing on this basis the phenomenological laws of heat transfer between the heat well and heat sink with temperatures of  $T_h$  and  $T_c$  and the working medium in the cycle as:

$$T_h - T_1 = R_h J_q'; \quad T_2 - T_c = R_c J_q''. \quad (19.5.5)$$

where  $R_h$ ,  $R_c$  – overall thermal resistance to heat exchange from the heat well and heat sink, respectively, easily gives that the temperature drops from the heat well and heat sink are related with the thermal resistances thru the relationship:

$$(T_2 - T_c)/(T_h - T_1) = (1 - \eta_t) R_c/R_h. \quad (19.5.6)$$

Expanding the expression of  $\eta_t$  a relationship between the temperatures of heat application and abstraction can be easily obtained (V. Etkin, 1991):

$$T_2 = T_1 T_c / [T_1 (1 + R_c/R_h) - T_h R_c/R_h]. \quad (19.5.7)$$

This relationship existing demands a correction of the conditions under which the peak cycle power can be obtained. Let us consider for example the problem of determining the optimal (at peak power conditions) heat application temperature in cycles of a nuclear power plant (NPP) on saturated steam (Calafati, 1963). Let the heat pick-up from a light-water nuclear reactor  $J_q'$  be restricted by the temperature  $T_{max}$  of the fuel elements. Then the theoretical power of the plant  $N_j$  defined as the product of the heat flow  $J_q'$  from the heat well by the thermal efficiency of the NPP cycle  $\eta_t = 1 - T_2/T_1$ , where  $T_1$ ,  $T_2$  – mean integral temperatures of heat application and abstraction, respectively, in the NPP cycle, will have a peak due to efficiency deterioration as the heat flow from the heat well  $J_q'$  increases. Let us assume after the work mentioned that the temperature averaged over the heat exchange surface is identical to the mean integral temperature  $T_1$  of heat application to the working medium (so that  $J_q' = (T_h - T_1)/R_h$ , where  $T_h$ ,  $R_h$  – mean integral temperature on the surface of the fuel elements and thermal resistance to the heat transfer from the heat well to the working medium, respectively). Let us also assume that the coefficient of heat release and temperature distribution variation over fuel

element height  $k_p = (T_h - T_1)/(T_{max} - T_1)$  does not depend on power. Then the NPP power will be:

$$N_j = J_q \eta_t = k_p (T_{max} - T_1) (1 - T_2/T_1)/R_h \quad . \quad (19.5.8)$$

Considering this expression as a function of the initial cycle temperature  $T_1$  and allowing for relation equation (19.5.7) after a number of transformations with constant  $T_h$  and  $T_c$  gives the optimal heat application and abstraction temperatures in peak power cycles (Etkin, 1997):

$$T_1^{opt} = (\sqrt{\overline{T_h T_c}} + T_h R_c/R_h)/(1 + R_c/R_h) \quad , \quad (19.5.9)$$

$$T_2^{opt} = (T_c + \sqrt{\overline{T_h T_c}} R_c/R_h)/(1 + R_c/R_h) \quad . \quad (19.5.10)$$

These expressions differ from those obtained in finite-time thermodynamics in the degree of the  $R_c/R_h$  contagion. It may be easily found that this ratio features the interrelation between the heat application and abstraction temperatures in an arbitrary cycle. In fact, considering  $T_2$  as a function of  $T_1$  and differentiating (16.5.10) under the  $R_c/R_h$  constancy with  $\eta_t^{opt}$  independent on this ratio gives:

$$\partial T_2/\partial T_1 = -R_c/R_h (1 - \eta_t) \quad . \quad (19.5.11)$$

From this it follows that the relation degree between the heat application and abstraction temperatures  $T_1$  and  $T_2$  is defined by the  $R_c/R_h$  ratio. To illustrate how it is important to take into account the relation between initial and final parameters for the power plant optimization, let us consider a specific example of determining the optimal heat application and abstraction temperatures in NPP cycles with water-cooled reactors, for which, due to the minor  $c_r$  value, the peak power operating conditions are most economically advantageous (Calafati, 1963). However, unlike the traditional approach to determination of the NPP peak power cycle initial parameters based on the usual assumption of cycle heat abstraction temperature  $T_2$  constancy, we will proceed from expression (16.5.11). In the calculations following the author mentioned the maximal temperature of the fuel elements made of metallic uranium is adopted as  $T_{max} = 928$  K (650°C) and  $T_2 = 302$  K, which according to (19.5.2) gives the value  $T_1^{opt} = \sqrt{T_{max} T_2} = (928 \cdot 302)^{0.5} = 528$  K. Like in the work mentioned, it is assumed in the calculations that the coefficient of temperature distribution variation over fuel element height with cosine heat release distribution  $k_p = 2/\pi$  does not depend on power, which corresponds to the mean integral

temperature of the fuel elements as the heat well  $T_h = 782.8$  K. The results of such calculations for various  $R_c/R_h$  ratios are shown on Fig.19.4.

As follows from the figure, the optimal heat abstraction temperature considerably exceeds its usually adopted level already at enough low values of  $R_c/R_h \approx 0.05 \dots 0.08$  typical for NPP. As the  $R_c/R_h$  ratio increases, the gap becomes especially noticeable. This fact evidences the necessity to jointly assign the initial and final cycle parameters of a power unit considering their relation. This interrelation becomes especially important for spacecraft power units where the heat abstraction into the ambient space is provided by radiation, while the  $R_c/R_h$  ratio increases by almost two orders. To confirm the said, let us consider a particular

example of the American orbital station elaborated by General Electric (Favorsky and others, 1970). Its steam turbine power unit comprises a nuclear reactor with a thermal power of  $N_T = 8$  MW, a steam turbine in complete with a generator with a net electric power of  $N_e = 1$  MW and a finned-tube radiator cooler. The power unit features two main liquid-metal circuits. Liquid lithium is the working medium of the first circuit, while potassium – of the second one. The temperature of the potassium entering and leaving the turbine is  $1,065^\circ\text{C}$  and  $704.4^\circ\text{C}$ , respectively. The maximum allowable temperature of the fuel element is  $1,221^\circ\text{C}$  and the temperature of the potassium entering and leaving the reactor is  $1,037.8^\circ\text{C}$  and  $1,093.3^\circ\text{C}$ , respectively, which corresponds to the mean integral heat application temperature thru cycle  $\bar{T}_1 \approx 1,324$  K. The cycle thermal efficiency  $\eta_t$  corresponding to the heat abstraction temperature  $\bar{T}_2 = 977.5$  K is equal to 0.26. The equilibrium temperature of the radiator cooler  $T_c$  (in the absence of  $Q_2$ ) found from the heat balance between the solar radiation flow onto the radiator cooler surface and the heat abstraction from the radiator cooler into the ambient space by radiation is tentatively 750 K. At these conditions the  $R_c/R_h$  ratio found from expressions (19.5.6) is equal to 2.1–2.2, which exceeds by two orders its value usual for ground thermal power plants. Optimal heat application and abstraction temperatures found for these parameter values from (19.5.6)–(19.5.7) are  $\bar{T}_1^{opt} =$

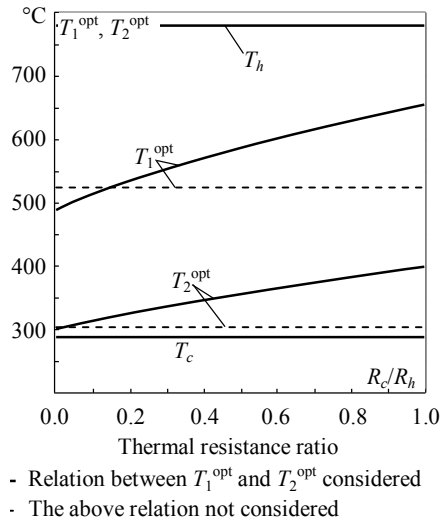


Fig.19.4. Interrelation between Heat Application and Heat Abstraction Temperatures in NPP Cycles with Water-Cooled Reactors

1350 K and  $\bar{T}_2^{opt} = 960$  K, respectively – quite close to their true values. At the same time it is noticeable that the plant cycle heat abstraction temperature appears to be 210°C higher than the conditional temperature of the sink. This stresses the necessity of interrelated search of optimal heat application and abstraction temperatures in the cycles of power units.

The examples considered herein evidence that thermokinetics substantially expands the applicability of finite-time thermodynamics allowing not only to extend its methods to systems with various value of optimal load, but also to clarify a number of its deductions.

## Chapter 20

### TO USING FIELD FORMS OF ENERGY

“...It is just a matter of time,  
how soon mankind will succeed in  
connecting its machines to the very  
power source of the ambient space”

N. Tesla

Matter is known to exist in two forms, viz. substance and field. Up to date mankind have used the energy of only the former of them. Such are, in particular, the chemical energy of fuel and the nuclear energy of spontaneously fissionable elements. The final product of the substance energy conversion is in most cases a substance in its modified state, which is accumulated on the planet directly endangering its ecological stability. The problem is aggravated by the concentration of population within huge megapolises and by increasing consumption of energy resources. The energy generation has become increasingly centralized, hydropower dams and thermal power plants have become increasingly gigantic, oil and gas pipelines, as well as power transmission and heat supply lines – increasingly extended. This just facilitates an ecology crisis and aggravates the consequences of natural disasters. Fossil fuel resources are being depleted, while the share of renewable energy sources remains extremely low. In search of new energy sources the scientific community takes the ever growing risk postponing for an uncertain time the solution of the problem of nuclear waste disposal and conservation of the exhausted nuclear plants. Vast funds are being spent to harness the thermonuclear reactions. It seems as though there is no a way out of the situation.

Meantime, in the present circumstances mankind ought to pay closer attention to such alternative forms of renewable energy as the energy of the field forces surrounding us.

### 20.1. Theoretical Possibilities of Creating Alternators

According to information received to date there are more than couple of tens of devices in operation with an output exceeding the measurable input, and more than a hundred of patents granted for such devices in different countries. Such devices are often called the “free energy generators”, “over-unity devices” (with efficiency in excess of 100%), “surplus power generators” and even “perpetual motion machines”. The authors of such publications are not willing for various reasons to recognize the energy sources not estimable by present-day means. It comes down even to the fact that the ambient energy consumption is neglected just due to the absence of...the tangible costs associated. This can not be justified by whatever considerations, the more so because all renewable energy sources feature low expenses.

Since the physical content of these terms absolutely violates energy conservation, it should be rather construed that such devices would use unaccounted energy sources alternative to not only conventional organic and nuclear fuels, but also to renewable energy sources. Therefore they will hereafter be termed *alternators*<sup>1)</sup> for short. However, the authors of publications for various reasons do not wish to recognize as energy sources those inestimable by modern means. It comes down to even disregarding the energy from unknown sources because of unavailability... of the tangible costs associated.

At these conditions it looks like reasonable that alternators be analyzed via application of thermokinetics which body of mathematics, unlike the cycle method of classic thermodynamics, operates exclusively parameters of energy converting system itself rather than energy (heat) sources. It is just apropos for alternators since the energy sources and their streams, as well as their parameters, remain unknown in most cases.

According to thermokinetics, for thermodynamic analysis of an arbitrary machine converting some  $i^{\text{th}}$  field form of energy into the  $j^{\text{th}}$  form, the law of energy conservation (2.4.9) should be used, which for the case of vector forces acting gives:

---

<sup>1)</sup> The term “alternators” refer presently to the only class of the “over-unity devices”, viz. magnetic motors and generators. We will refer to it in the wider sense.

$$dU = \bar{d}Q^d - \mathbf{X}_i \cdot d\mathbf{Z}_i - \mathbf{X}_j \cdot d\mathbf{Z}_j = 0. \quad (20.1.1)$$

This equation differs from the Gibbs' generalized relationship (2.3.1), the classic thermodynamics operates since it does not contain the terms  $\Sigma_i \Psi_i d\Theta_i$  describing transfer of the energy carrier  $\Theta_i$  across the system borders and, on the contrary, contains the term  $\bar{d}W_j = \mathbf{X}_j \cdot d\mathbf{Z}_j$  describing the work done by the force field and working medium itself. In the particular case of electrical and magnetic fields the parameters  $\mathbf{X}_i$  and  $\mathbf{Z}_i$  refer to the working medium, while the parameters  $\mathbf{X}_j$  and  $\mathbf{Z}_j$  – to the object the work applies to. The terms  $\mathbf{X}_i \cdot d\mathbf{Z}_i < 0$  and  $\mathbf{X}_j \cdot d\mathbf{Z}_j > 0$  characterize here, respectively, the work done on the working medium by the force field and the work done by the working medium itself on the object the work applies to; the term  $\bar{d}Q^d$  describes the elementary dissipation heat released for the time  $t$  within the system volume  $V$ . As can be seen, to analyze the cycle involving a non-equilibrium working medium, there is no need to know the parameters of the energy source. This makes it possible to analyze the processes running in energy converter without knowing the parameters of the energy source. Such an analysis, as shown in Chapters 15 and 16, includes finding the motive forces  $\mathbf{X}_i$ ,  $\mathbf{X}_j$  and the energy carrier flows  $\mathbf{J}_i$ ,  $\mathbf{J}_j$  for energy forms being and having been converted, formulating the laws of energy conversion (18.4.1...18.4.2) in a particular machine, finding the similarity criteria (18.4.6...18.4.7), determining the power efficiency of the machine and revealing the deviation of its operation from optimum for this particular type of energy converters. These problems outstep the classic theory of heat engines.

Unfortunately, such an analysis does not give a unique indication of energy source. However, as shown in Chapter 16, with regard to renewable energy sources for which investments do not noticeably contribute to the net cost of the energy generated, their consumption is not of fundamental importance. Therefore the alternators are to be considered as ranked with other machines operating on renewable energy sources. However, the fact should not be left out of consideration that a field form of energy, from the positions of thermokinetics, is caused by heterogeneous distribution of “field-forming” material objects in space and, therefore, belongs to them, but not to space itself (ether or physical vacuum), whatever properties we may try to attribute to this space. It remains to show that whatever “free energy generation”, “surplus power” and “over-unity efficiency” are out of the question. To do so, the equation (20.1.1) is easier to be represented in the form of the energy balance equation

$$dU/dt = N_i - N_j - N^d. \quad (20.1.2)$$



Here  $N_i$  means the power input to the alternator;  $N_j$  – net power of the device;  $N^d$  – dissipation power in the system. From here the power efficiency expression ensues, which for cyclic machines ( $dU/dt = 0$ ) according to (18.2.9) takes the form:

$$\eta_N = N_j/N_i = 1 - N^d/N_i \leq 1. \quad (20.1.3)$$

Thus the efficiency of any real energy converter (with  $N^d/N_i > 0$ ) is always below unity, i.e. the work of alternators is always done in strict compliance with the laws of thermodynamics and without violation of its first law.

The energy exchange arising between matter and field explains the functioning of alternators without recourse to whatever hypotheses and postulates lying beyond the existing scientific paradigm. Such a position basically differs from the opinion common for both the traditional academic ambience and alternative scientific forums which declare that, to substantiate the principle of operation and to develop the “over-unity” devices (with efficiency  $> 1$ ), some novel “exotic” branch of physics is needed.

The further thermokinetic analysis of the alternators is advisably to be conducted in application to a particular type of working medium that provides the energy conversion in some of the stationary force fields. Hereafter we will consider examples of the energy converters for the force fields known, viz. gravitational, electrostatic and electromagnetic. Such a consideration is basically aimed at demonstrating the fact that the alternators follow the unitary thermokinetic laws of energy conversion.

## 20.2. Gravitational energy Converters

The idea to create the “perpetuum mobile” (perpetual motion) technical devices is rooted in philosophy of the Ancient Orient. This is the place wherein the first documentary evidences about the creation of a gravitation-based engine originate. Such is, in particular, the Bakhaskar “self-rotating wheel” (India) with tubes tangentially arranged and half-filled with water, which demonstrated in mid 12<sup>th</sup> century. In Europe the first projects of such mechanical “perpetual motion machines” appeared in the 13<sup>th</sup> century: the V. Honnecourt’s wheel with seven weights (France, 1245), the similar V. Maricourt’s wheel (France, 1269). Leonardo da Vinci left a number of drawings behind him with a device where vertically falling weights or water rotated a wheel and thus worked efficiently. Mariano di Jacopo built in Italy (1438) a system of eight rods radially ar-

ranged in the plane of rotation and all bendable in one direction. Due to this fact the left half of the system differs from its right half in weight, thus, providing the rotation. Cornelius Drebbel, alchemist and magician, created a perpetuum mobile in 1610 (presumably). Robert Fludd had developed a plenty of devices of such a type up to 1630. Later on in 1870 many people tried to obtain patents for Fludd's device variations. Ulrich von Carnach developed a "ball" perpetuum mobile in Germany in 1664. The famous scientist Jean Bernoulli (1667-1748) put forward a fluid-energy device project. Bockler designed a "self-rotating" mill in 1686 based on the Archimedes' screw in various versions.

In England the first perpetuum mobile patent was granted in 1635 for the E. Somerset's 4-meter wheel with 14 weights per 25 kg each. The machine was brilliantly tested in London in the presence of King Charles with a record available in the archives. One of such wheels E. Somerset demonstrated to the King of France in 1638. It is significant that already 600 patents for such devices had been granted in England up to 1903.

The wheel of J. Bessler (better known as Orffyreus) gained the most distinction in the early 18<sup>th</sup> century. For several tens of years he publicly demonstrated various models of his wheel set in motion with weights inside it, which developed an asymmetrical moment at wheel rotation. The last of his designs was 6 feet in diameter, 12 inches in thickness and rotated with a speed of 42 rpm. That wheel not only kept continuous rotation, but also allowed to do useful work, e.g. lifted a weight with a mass of 16 kg to a height of 1.5 m. Its operation was more than once scrutinized by famous scientists and officials, while German Prince Karl let into its design granted Orffyreus a certificate for "Perpetuum Mobile". Under control of a competent commission of 11 members (Professor Gravesaint, Newton's intimate friend, among them) the wheel kept working in a room locked and sealed up for 40 days and at a sudden inspection showed as-before rotation with a speed of 26 rpm. The tests repeated many times since the commission scrutinized the availability of secret drives (the reason wherefore the wheel changed its location).

As one can see, those were not charlatans at all who were occupied with perpetual motion machines. Therefore, it is hardly to credit of the Parisian Academy of Sciences, one of the highest authority at that time, that it resolved in 1775 (i.e. before the energy conservation law discovered) to exclude such projects from consideration. It is not out of place to note that still earlier that Academy had refused to consider the existence of meteorites as an absurdity of rockfall down from the heavens. It is well known what a confusion it caused. It is quite possible that if the French academicians had not disregarded a careful and unbiased consideration of such machines, power engineering and science in whole could have followed quite other path in their development. However, in reality an abso-

lutely opposite situation developed: when an operating machine pretending to be the “perpetuum mobile” was publicly demonstrated, no reasonable refutations followed, but usually the case closed, as for the Orffyreus’ wheel, with a magazine pamphlet.

Assuming that the task of real science is not at all the devotion to a paradigm having become antiquated long ago, let us consider, from the positions of thermokinetics, the operation of one of such devices, e.g. the Fraga’s wheel (Cuba, USA Patent IL60915,1987).

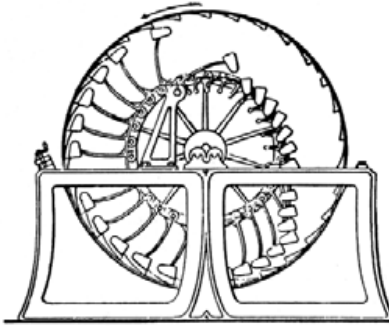


Fig. 20.2. Fraga’s Wheel

This device constitutes a self-rotating wheel with non-balanced weights secured at the ends of levers (Fig. 20.2). The opposite ends of the levers accommodate movable joints enabling the levers to “tilt” when transiting the unstable equilibrium point. The wheel has a number of cogs securing the weights with the levers till the position of the maximum possible torque (left part of the wheel). On the contrary, the weights in the right part of the wheel are always in the position of the minimum possible torque.

The device is induced to stable rotation by a minor push. For our case the basic equation of thermokinetics (2.2.5) has the form:

$$dU = TdS + \mathbf{F}_g \cdot d\mathbf{r}_g + \mathbf{M} \cdot d\boldsymbol{\varphi}, \quad (20.2.1)$$

where  $TdS = dQ + dQ^f$  – total heat the system receives from outside ( $dQ$ ) and releases due to friction ( $dQ^f$ );  $\mathbf{F}_g$  – gravity force;  $\mathbf{r}_g$  – center-of-mass radius vector of the wheel;  $\mathbf{M} = \mathbf{F}_g \times \mathbf{r}_g$  – torque applied to the wheel from gravitational field;  $\boldsymbol{\varphi}$  – angle of wheel rotation.

Comparing this expression with the combined equation for the first and second laws of classic thermodynamics (2.2.7) wherein the expansion work  $pdV$  is superseded by other (the  $j^{\text{th}}$ ) kinds of work  $dW_j$

$$dU = TdS - dW_j, \quad (20.2.2)$$

gives that, should a heterogeneous system have the internal energy of gravitational interaction between system parts, the term  $dW_j$  includes the weight displacement work  $\mathbf{F}_g \cdot d\mathbf{r}_g$  and the wheel rotation work  $\mathbf{M} \cdot d\boldsymbol{\varphi}$ .

Let us apply this equation to the circular process the Fraga’s wheel runs:

$$\oint dU = \oint TdS + \oint \mathbf{F}_g \cdot d\mathbf{r}_g + \oint \mathbf{M} \cdot d\boldsymbol{\varphi}. \quad (20.2.3)$$

This expression can be essentially simplified given the circuital integral of any state function, including system energy, equal to zero ( $\oint dU = 0$ ) and the friction and external heat exchange neglected ( $\oint TdS = 0$ ). Furthermore, since the gravity force  $\mathbf{F}_g$  remains essentially invariable in circular process, then factoring  $\mathbf{F}_g$  outside the integral sign and given  $\oint d\mathbf{r}_g = 0$  gives that the second term on the right-hand side also becomes zero. Thus, from the positions of Newton's mechanics not catering for rotational motion (in the absence of the term  $\oint \mathbf{M} \cdot d\boldsymbol{\varphi}$ ), the Fraga's wheel should be attributed to the "perpetual motion of the first kind". However, considering the third term on the right-hand side of (20.1.3) gives immediately that the Fraga's wheel cycle work  $W_c = \oint dW_j$  is equal to

$$W_u = \oint \mathbf{M}_g \cdot d\boldsymbol{\varphi}_g \quad (20.2.4)$$

This expression shows that the cycle work of gravitational converter may differ from zero if gravitational field does work for rotation of the wheel. This work may differ from zero since the field of torques is not potential. Let us now clarify the conditions making this work other than zero. To do so, divide circuital integral (20.1.4) into parts 1–2 and 2–1 wherein the angle  $\varphi$  varies from 0 up to  $180^\circ$  and from  $180^\circ$  down to 0. For the sake of simplicity represent the integrand (20.1.4) in terms of scalar values of  $M$  and  $\varphi_g$  and denote the torque and rotation angle for these parts of the cycle with single or double stroke, respectively ( $M'$ ,  $\varphi'$  and  $M''$ ,  $\varphi''$ ). Then based on (20.2.4) and given the opposite signs for the torques on these parts ( $M'' = -M'$ ) one may write down instead of (20.2.4):

$$W_u = \int_1^2 (M' - M'') \cdot d\varphi_g' \quad (20.2.5)$$

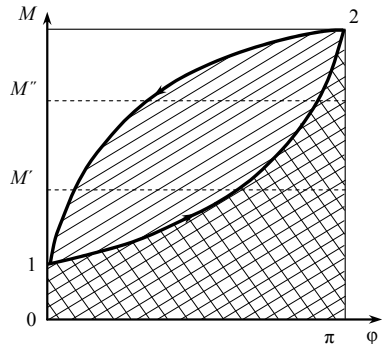


Fig. 20. 3. Cycle of Unbalanced Wheel in Gravity Field

The  $M-\varphi_g$  cycle of such a device for one of the weighted levers is plotted in Fig. 20.3. Let us assume that at initial time this weight takes the extremely lowest position (angle  $\varphi$  makes  $0^0$  to vertical). With an external force applied let us turn the wheel counterclockwise at an angle of  $180^0$  so that the weight arm  $r_g'$  remains minimal (process 1–2). This action is associated with an external work exerted and expressed by the cross-hatched area. With the apex position reached a weight “throw-over” will



Fig. 20.4. A. Kosta's Wheel

occur and the further rotation of the wheel will proceed as a self-motion (process 2–1). The self-motion work expressed by the hatched area under curve 2–1 will exceed the exerted work due to increasing  $r_g''$  and the corresponding average torque  $M''$ . The weight lift along 1–2 will further continue without an exerting interference since the average counter-torque  $M''$  will be lower. This is the principle of operation of the self-rotating wheels which do not thus violate whatever laws of physics and are not the “perpetual motion” in the common sense of this term. It remains only to show that the operation of such a device follows the same universal load curves as the other engines. In our case the forces  $\mathbf{X}_i$  and  $\mathbf{X}_{i0}$  are construed as the moments  $\mathbf{M} = \mathbf{g}r_g$ , so the load criterion take the form  $B = 1 - r_g'/r_g'' < 1$ . As for the Q-factor  $\Phi$ , it remains unknown. However,

given the wheel friction, it is certainly below infinity, so from the curve in Fig. 20.2 it follows that the power efficiency  $\eta_N$  and the engine power  $N$  become zero at the balance of arms  $r_g' = r_g''$  which is in strict compliance with experiment. From this it also follows that the device should be tuned to find the optimal relation  $r_g'/r_g''$  – the fact as well noted by the inventors of these devices. It remains only just to instantiate the above with several present-day designs of such devices. One of the most impressive machines of such a kind is the device (Fig. 20.4) A Kosta built (Patent France No95/12421, 1995). His 18-meter unbalanced wheel is the best wordless evidence of the inventor's earnest approach and confidence in

integrity of the design he has created. This wheel operates to the same principle and contains 236 movable elements providing its rotation. It can rotate both clockwise and counterclockwise. As the inventor notes, the main problem of its fabrication was to reach the variation of the mass positions “in proper place and at proper time”.

In 2006 the power company Envision announced its readiness to bring to the market a generator SPEGG producing electric power without fuel consumption. The generator is a self-rotating wheel Warranline that is coupled to a current generator and has 16 spokes (Fig. 20.5). Eight of them contain weights being in translation movement and thereby compressing springs.

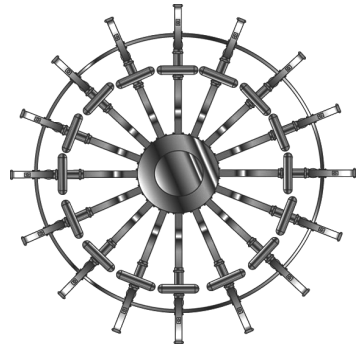


Fig. 20.5. Warranline Wheel

The wheel is designed so that it is always heavier on one side. This disturbs its equilibrium in gravity field forcing it to rotate. Thus the great idea to use inexhaustible “living forces” of nature is starting to take real shape.

### 20.3. Generators Using Electrical Field energy

Let us now consider the generators using the energy of the natural electrostatic field. The Earth and its ionosphere are known to constitute a “spherical condenser” which energy content according to recent calculations (E. Rauscher, 2002) is about  $3 \cdot 10^9$  kWh with a capacity of  $15 \cdot 10^3$   $\mu$ F. The intensity of the electrostatic field it generates averages 100 V/m. This gives hope to mankind, according to N. Tesla, “to connect its machines to the very power source of the ambient space”. One of the possible designs he offered looks like an antenna in the form of a metalized balloon lifted above the ground and serving as an electric charge integrator. Being connected to an energy converter through a cable, this integrator is capable to use the “gratis” energy of atmospheric electricity. J. Swenson has conducted a series of simple experiments aimed at “energy recovery from air”. Natural electrical oscillation frequency of the planet, as known yet from Tesla’s time, is 7.5Hz. Swenson dealt with a resonance frequency of 375 kHz and a 10-meter antenna (Fig. 20.6). This version of the energy recovery from the ambient space has been implemented in the Efimenko’s electrostatic generator described in the book “Electrostatic Motor” (1973). A cylindrical rotor rotates in the potential electrical field generating a power of about 70W by means of a usual dy-

namo. The electrical field of the Earth serves as a field source (6,000W), for which reason the machine has an antenna and grounding. Such machines using the potential difference between the planet surface and ionosphere have been known yet from 1800's. In this case not just posing a problem, but its solution is of interest.

In a number of cases the electrostatic fields can be generated artificially,

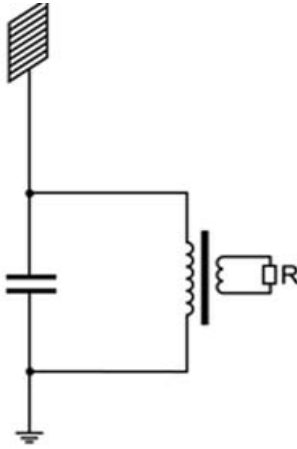


Fig. 20.6. Swenson's Generator Schematic

which has been proven by the energy generator Testatica invented by P. Bauman and built in the Methernita Christian community. Several of such fuel-free generators have produced for 30 years an electric power of 750kW covering the entire community's demands (including also the workshops located in the same place). From the technical standpoint this device is the Wimshurst modernized influence machine. The machine features two discs with steel or aluminum segments fixed to the discs. The separation of the charges on the disc segments occur due to the brush friction. The brushes also pick up the charges on the disc segments. The self-rotation of the discs is provided by, evidently, the mutual repulsion of the wheel segments rotating in the opposite directions due to delay of the electrostatic interaction forces. The reaction force in this design can decrease by the relative displacement of the brushes assuring decreasing the charge on the segments at the moment the segments are drawing together. Such a machine with a disc diameter of 20 cm generates a power of about 200W; the large-scale machine has discs with a diameter of 2 m and generates about 30kW of power. A special diode module and Leyden jars provide frequency regulation. The design also includes permanent horseshoe magnets with coils connected to the Leyden jars and intended to maintain the frequency due to resonance, as well as a device stepping the voltage from 100kV (and more) down to 200V. Using permanent horseshoe magnets in the modern converter version is noted to considerably increase EMF.

In this aspect it is much more promising to use "electrodynamic" effects associated with the pulsed operation of devices using natural electricity. Yet N. Tesla, when conducted experiments with high-voltage DC generator, spark discharger and high-voltage air-core transformer (Tesla transformer) in the ninetieth of the 19<sup>th</sup> century, noticed a considerable increase in the power the device released into the environment against the high-frequency AC generator with a conventional step-up transformer.

In this aspect it is much more promising to use "electrodynamic" effects associated with the pulsed operation of devices using natural electricity. Yet N. Tesla, when conducted experiments with high-voltage DC generator, spark discharger and high-voltage air-core transformer (Tesla transformer) in the ninetieth of the 19<sup>th</sup> century, noticed a considerable increase in the power the device released into the environment against the high-frequency AC generator with a conventional step-up transformer.

Tesla called that power increment “radiant electricity” having attributed it to ether and opposed to the conventional electric current as an electron stream. That statement was based on the effect Tesla discovered, which generated a voltage spatially distributed. The latter grew along the secondary coil length of his non-electromagnetic transformer and might thousands times exceed the spark discharger initial voltage and not to be proportional to the number of ampere-turns (since there was no current in the winding). That “electro-radiant” effect appeared when the high-voltage direct current was discharging to spark gap and broke before the back (reverse) current appeared. The effect intensified with a capacitor included in the high-voltage DC power supply. The energy flux caused by that effect spread in the form of a longitudinal electrostatic “light-like” beam that moved perpendicularly to the coil turns like incompressible gas under pressure and did not penetrate into the conductor. Fast interruption of direct current with magnetic interrupters generated a shock wave in the laboratory wherein the Tesla transformer was installed. This wave might be sensed as a sharp shock and an electric discomfort (“tickle”) that, unlike the conventional electromagnetic radiation, penetrated through metal shields and most of dielectrics. Nevertheless, the pulses the Tesla transformer radiated, when shorter than 100 microseconds, were absolutely harmless to people and did not cause heating. The magnitude of those pulses depended on their duration and on the spark discharger voltage. They generated light effects in the vacuum tubes and caused a “response” in metals in the form of electric charge accumulation.

Thomas Henry Moray (USA) was among the Tesla’s followers. In 1909–1910 he created a number of devices operating, as he believed, on electrostatic charge of the Earth and ionosphere. One of such demonstrational devices was represented to experts for review (with the exception of a small box that the author preferred having kept in his breast pocket). The device consisted of capacitors, step-up transformer, spark discharger and a panel with two radio tubes, as well as of a permanent magnet, switchers and lamps of 100W and 20W as a load. Whatever batteries were absent in the device, however, the design included antennas with a length of up to 200 feet elevated about 80 feet and a grounding deepened about 7 feet. The device was tested for a time period lengthy enough at both home conditions and in the mountains (far from power transmission lines). Some of the devices developed a load power of up to 650W at a voltage of up to 250kV. As can be seen, there are many elements in this device similar to the Tesla’s technique.

Many of such elements can be revealed in the “over-unity” engine-generator of Edwin Grey (USA). For a period of 1961–1986 he built and patented several prototypes of self-sustained EMA devices (Electric Magnetic Association) capable to generate electric power without fuel used



and to supply the needs of an apartment house, automobile, train or plane. Repeated demos of his technique gained enthusiastic comments in the press, while Grey himself was honored with a title of “Inventor of the Year” (1979) and with the “Quality Certificate” from R. Reagan, who was the Governor of California at that time. Like the Tesla’s device, the Grey’s generator was powered with high-voltage direct current. However, instead of the high-voltage DC generator, a battery was used there with the output interrupted through a multi-vibrator. The pulses from the multi-vibrator were delivered to the primary coil of a conventional transformer with the high-voltage winding connected to a bridge-type rectifier. Like in the Tesla’s device, the high-voltage DC power supply periodically charged a high-value capacitor. The spark discharger was one more mutual component. However, instead of the transformer, the Grey’s device used an “electrical conversion switching element tube” which consisted of a resistor, spark discharger and “charge receiving plates”, i.e. combined three components of the Tesla’s device. It was the electrical conversion switching element tube that did work when powered an engine, TV set, radio set, incandescent-filament lamps, etc. The “cold electricity” circuit, as Grey called it, operated likely in the following way: the storage battery voltage was stepped up to 3,000 V and stored in a high-value capacitor. Then the pulses discharged through a spark gap governed by electronic tubes so that the pulse duration was less than 50 microseconds. That intermittent pulse sequence passed through the conversion switching element tube where was entrapped on the charge receiving plates. The load was provided as a transformer that stepped the voltage down to power the electronic tubes and other loads, as well as an additional step-down transformer to charge a secondary battery. Having the batteries periodically switched, Grey not only recovered the power supplied, but also received an imposing “surplus” power. Nevertheless, all his attempts to apply his technique for commercial purposes failed. In the late 1970th the company Zetec, Inc. bought up the Grey’s technology, while the inventor’s attempts to intrigue the US Government and Senate in his work were not responded. Edwin Vincent Grey died in April 1989 in his workshop in Sparks (Nevada) at the age of 64 under the mysterious circumstances.

However, ideas never die without leaving a trace, which is once again confirmed by the Testatika energy generator invented by Paul Baumann and built in the Methernita Christian community (Switzerland). Several of such fuel-free generators have produced for 30 years an electric power of 750 kW covering the entire community’s demands (including also the workshops located in the same place). Like in the case of E. Grey, the idea was suggested to P. Baumann through studying lightning. Unlike Tesla and Grey, to obtain a high-voltage DC source, the Wimshurst (1832–1903) generator was used, which application was practically

ceased with electromagnetic generators introduced. The Wimshurst generator consisted of two discs which rotated in the opposite directions and had steel or aluminum segments fixed to them. The separation of the charges on the disc segments occurred due to the brush friction. The brushes also picked up the charge on the disc segments. The charge then drained into the Leyden jars and stored there. In the Testatika (see Fig. 20.7) the high voltage from these capacitors is supplied to the top of large metallic jars (which contents P. Baumann never showed to anyone and which caused a lot of guess-work – from capacitors with uranium additives and to a fancy crystals–magnets combination) and then removed out of the bottom to spark dischargers. In the figure two permanent horseshoe magnets can be seen along with the spark dischargers. Thus the

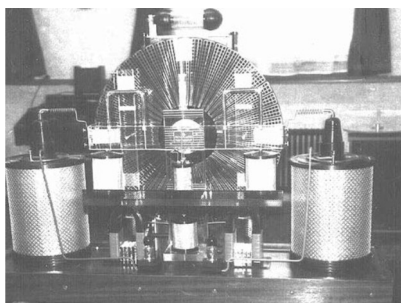


Fig. 20.7. Testatika Generator

Baumann’s generator uses the same elements to enhance spark formation and arc breaking as in the Tesla’s machine.

The self-rotation of the discs after an initial impact is provided by the mutual repulsion of the segments in two wheels due to the forces of electromagnetic interaction since the rotating electrified disc of the generator forms together with the external circuit

a high current loop where the current runs in the discs in the opposite directions. Electrostatic repulsive forces may also take part in the process. The rotation is adjusted by a relative displacement of the brushes. A prototype of such a machine with a disc diameter of 20 cm generated a power of about 200 W. The large-scale Testatika machines have discs with a diameter of 2 m and generate about 30 kW of power. A special diode module and the Leyden jars provide frequency regulation. The design also includes a device stepping the voltage from 100 kV (and more) down to 200 V.

The fact the machine exists and operates is confirmed by the reports available from 12 recognized scientists who visited the community at different times to investigate and check the Testatika integrity (including Prof S. Marinov, who built working models of the generator and finally perished under the mysterious circumstances). All of these reports come to the recognition of the fact that the principles of Testatika’s operation remain obscure.

The William Hyde’s device (Patent USA No4897592, 1987) is one of the operating up-to-date designs close to the Baumann’s machine in its technical solution. The author called it a “system generating power from

electric field”. It includes conventional elements of an electrostatic generator using rotating discs with segments like in the Swiss M-L converter Testatika. In the prototype of 1987 Hyde used up to 240 rotor segments and 480 stator segments. His generator rotates with a speed by an order of magnitude exceeding the Testatik speed. Furthermore, Hyde supplemented his design with several new elements, viz. stator discs on electrode plates, external 3 kV-power supply charging these electrode plates, etc. With such a potential the pulse voltage on the stator reaches 300 kV. The double rotor discs in his machine rotate in the same direction. Due to this fact the paired stator segments appear to be periodically screened against the polarizing effect of the exciter. Each stator segment in the machine is electrically coupled with its pair through a circuit where the pulse voltage is reduced and rectifies for the output circuit. To accelerate the machine rotor, Hyde uses the potential electrostatic field on that path of the process where the field work is positive. Where the field decelerates the rotor, Hyde partially shields it. So an unbalance of the forces  $F_i$  and  $F_i''$  is created demanded by thermokinetics and allowing to obtain the energy from the stationary field source. The generator output is 22.9 kW with an input of 2.4 kW and a total load power of 20.5 kW. Due to its features, as well as to its description available, the self-rotating electrostatic Hyde’s generator is one of the most attractive alternator designs.

One of the recent domestic designs is worthy of notice – the hydromagnetic dynamo by O. Gritskevich – patented yet in 1988 in the USSR as a “method of generation and electrostatic plasma generator as its embodiment”. Considering our planet as a huge electrostatic generator the inventor offered a method to convert the force field of the planet into useful energy. The method was based on known physical principles, but used unique design solutions. The “non-mechanical” dynamo by Gritskevich was configured as doughnut-shaped bread roll with water as the rotor. Those generators agnominated as “water-warmers” had no pumps and none of the rubbing parts. They were operable for years practically without maintenance and not consuming even a gram of fuel. At the same time they were compact to be accommodated in any house and even a car. The cost of energy they generated was fortyfold lower than by a nuclear power plant, twentyfold lower than by a thermal power plant and fourfold lower than by a wind motor. The first prototype successfully operated in the mountains of Armenia and supplied the on-site needs of a scientific research station. However, despite the Rospatent certification and approval of scientific community, the hydromagnetic dynamo by Gritskevich has not found the market demand neither in Russia nor in the USA, where the inventor and seven of his mates from the design bureau emigrated in the late 1999. This circumstance evidences ones again that the main point here is not only the scientific consistency of the alternators

pertaining to this class and even not the search of their most promising design solutions, but the geopolitics of the energy park holders.

#### **20.4. Current Generators Using Magnetic Field energy**

The current generators based on permanent magnets constitute the most numerous and diversified class among the devices attributed to the “perpetual motion” category. The capability of the permanent magnets to do useful work (e.g. to lift metallic objects) has been known since several centuries ago. Since that time enthusiastic individualists have endeavored to use them. Yet seven centuries ago P Pilgrim offered the first magnetic engine. In the 16<sup>th</sup> century Jesuit priest J. Taisnerius was possessed with idea to create a magnetic “perpetuum mobile”. Later on the number of such projects rose to an avalanche and to date has reached such a scale that it becomes possible to introduce a branched classification of such devices by various criteria. The specific category of USA patents granted under the presentation of an acting model of the device claimed is the official confirmation of the integrity of some of the devices. Therefore, it is a matter of interest to demonstrate that the alternators of this class do not either violate whatever laws of thermokinetics and are attributed to the “over-unity” devices just through misunderstanding.

The magnetism of substances is known to be caused by basically the orbital motion of electrons, as well by their spin magnetic moments. Each of the magnets has its own “magnetic ordered energy” content, i.e. a kind of the “energy capacity” measured by the work which the magnet can do before its “depletion”. This capacity is highest for the relatively expensive magnets made of rare-earth metals, whereas much lower for the magnets made of the Alnico alloy.

The fact that magnets, in a great number of cases, do not lose their properties when doing work may be explained by only their “charging” from the ambient space. It is found that the permanent magnets, if shielded from the ambient space with a magnetic screen, will “deplete” much sooner in their operation under load. This will be confirmed hereafter based on the testing the Perendev Co’s magnetic engines. In operation without load, as long-duration tests show, permanent magnet coercive force changes negligibly (from zero for the rare-earth magnets throughout 3% for the Alnico magnets for  $10^4$  test hours). This supports the idea that if a permanent magnet is kept far from power supply lines, other magnets, high temperatures and other factors affecting it adversely, this magnet will forever preserve its magnetic properties. Shocks and vibrations do

not affect the modern magnetic materials unless and until they physically damage them.

The temperature of magnets dropping is a sure evidence of disturbing equilibrium between the electromagnetic field and the permanent magnets operating under load. This effect has been discovered in all without exception operable machines on permanent magnets. In the Floyd generator that temperature drop reached 20°C. The energy exchange between permanent magnets and the ambience is not evidently restricted to the thermal radiation range. All bodies interpret the nonthermal radiation as work done on them. Such phenomena as photoeffect, photosynthesis, etc. evidence this. It is also known that the magnetic induction depends on the area electrons “cover” in their orbital movement and may not only decrease in the process of radiation or the work the permanent magnet does, but also recover in the process of electromagnetic wave absorption increasing the energy of the orbital electrons. Thus the “mechanism” of such energy exchange is in general known: this is the absorption of energy of various-frequency electromagnetic oscillations or some “radiation” energy differing from the directional flow of photons (radiant energy) by its isotropic character. This energy may be attributed to oscillations of the ether as an all-penetrating medium which stressed state causes the existence of the force fields. However, from the positions of thermokinetics as a non-hypothetic theory it does not matter. What really matters is only that in any case the admissible continuous power of magnetic engines is limited to the rate of their energy exchange with the power source. This means that, from the positions of thermokinetics, the permanent magnets should be treated in the same way as any other working media running through a cyclic process, and whatever “perpetual motions” are out of question. In this case the operation of the generators on permanent magnets may be shown as based on the same mechanisms as for other heat and non-heat engines. To this end let us use the basic equation of thermokinetics (2.4.5) which in our particular case looks like:

$$W_{II} = \oint \mathbf{X}_M \cdot d\mathbf{Z}_M, \quad (20.4.1)$$

where  $\mathbf{X}_M = \mathbf{B}$ ,  $\mathbf{Z}_M$  – magnetic induction and magnetization of the magnet in whole, respectively.

Let us consider, as before, the scalars  $X_M$  and  $Z_M$  and divide the circular process into two parts, 1–2 and 2–1, in which limits the  $Z_M$  variation follows the same sign ( $dZ_M > 0$  или  $dZ_M < 0$ ). Then denoting  $X_M$  in “there” and “back” directions with single and double prime, respectively, and considering  $dZ_M'' = -dZ_M'$  gives instead of (20.4.1):

$$W_{II} = \int_1^2 (B_M'' - B_M') \cdot dZ_M' . \quad (20.4.2)$$

From this it follows that if the mean magnetic induction of a material is the same for both processes – its magnetization recovery ( $B''$ ) and doing work ( $B'$ ) – there will not be any work done for the cycle. The said is illustrated in Fig. 20.8, where an arbitrary cycle of a magnetic engine is depicted, which resembles the minor hysteresis loop.

The work for this cycle is defined by the cycle area. Hence, it is necessary to somehow change the character of the “there” 1–2 and the “back”

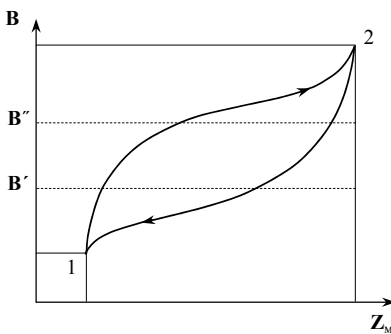


Fig. 20.8. Magnetic Engine Cycle

2–1 processes for the cycle area to become other than zero. This may be provided through e.g. Serl effect (magnet self-rotation), or temporarily shielding the magnetic field in-between the rotor and stator at the stretch where the magnets are closest to each other, or varying the magnetic induction in the rotor or stator by temporary variation of their temperature (nearby the point of phase transition), or varying the

path and field configuration when the rotor and stator magnets are moving to and off each other, or temporarily demagnetizing one of the magnets by electrical pulse at the moment of their opposition, etc. We will see hereafter these are the means the inventors of the permanent magnet-based devices of doubtless reality have recourse to.

The “Gramm’s generator” (Z.T. Gramm, 1869) is among the first of such devices. It features a rotating annular rotor with the toroidal coil touching two conducting brushes diametrically opposite. The rotor rotates within the poles of a stationary permanent magnet. The “asymmetry” of the magnetization and demagnetization processes for the annular rotor was provided by shifting the moment of voltage supply to the toroidal coil.

Later in 1996 Russian engineer A. Frolov upgraded the Gramm’s generator. His design features a stationary ring with coils, while one more coil in the center is used as the alternative magnetic field source (Fig. 20.9).

Two magnetic fluxes from the two load coils are mutually offset and, thus, there is no reaction in the primary circuit. This design concept has become popular (O. Berens, Sweden; D. Hofmann, USA; V. German, Germany; S. Hartman, USA; etc.). One of the designs based on this con-

cept and termed by its authors as “Frolov’s generator” is illustrated in Fig. 20.9.

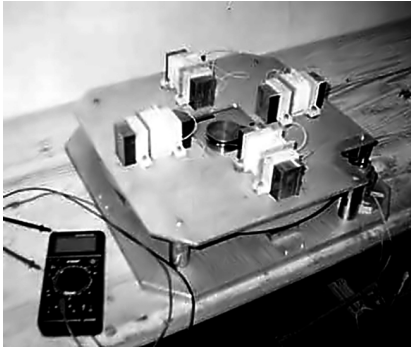


Fig. 20.9. Frolov’s Generator

The central permanent magnet is here set into rotation by a small-scale electric motor. To smooth the speed fluctuations, a massive flywheel applies (Fig. 20.9). In August 1999 V. German with his team in Germany succeeded to obtain more than 1,200W on load. In 2003 S Hartman (USA) designed a toroidal generator based on the standard 10kW-generator powered from a car storage battery. The generator input current was 0.8A at a voltage

of 12.92V, the output current was 40A at a voltage of 6.5V. Thus the power obtained was 25 times over.

John. Ecklin offered in 1975 another way of the “asymmetry” creation (Patent USA No3879622 dated 22.04.75). His engine features magnetic shielding and opening in turns and includes two permanent horseshoe magnets, a motor rotating “windows” – magnetic shields, and a magnet keeper of magnetic material, which is in turns attracted to one of the magnets not shielded at the moment. The keeper swaying transforms into the rotary motion through a crank gear. The patent notes that with field strengths, magnet forms and materials, etc. properly selected the energy obtained through the translation motion can exceed the one necessary to open and shut the “windows”. Ecklin did not manage to create a “self-starting” machine, nevertheless, his concept served as a basic for a number of USA patents: Jaffe (№3567979, 1976); Monroe (№3670189, 1976); E. Gray (№3890548, 1976); V. Rivas (№4006401, 1977); H. Johnson (№4151431, 1979); F. Richardson (№4077001, 1987); D. Regan (№4883977, 1989); V. Hyde (№4897592, 1990); H. Aspden (№4975608, 1990), etc.

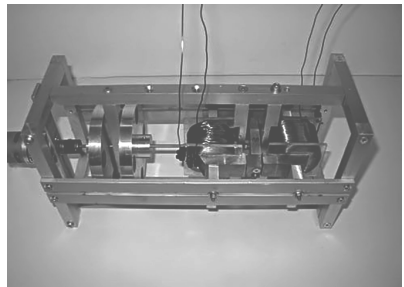


Fig. 20.10. German’s Motor

Some of the permanent magnets-based devices do not feature moving parts at all. The Vacuum Triode Amplifier (VTA) of S. Floyd’s design (USA) is one of them. Such a name is caused by the fact that the similar

principle of governing powerful flux through weak signal is used in triodes. In the VTA design barium magnets were used prepared by repeated magnetic reversal at a frequency of 60Hz. That facilitated the transit of the field from one direction to another when applying a weak signal to the control winding from an external generator, thus, providing its “trigger” operation. One of the VTA designs under demonstration included two sets of the (4×6×1)-inch magnets positioned against two walls of the casing in such an arrangement that an attraction appeared between them. The axes of the output windings were parallel to the field lines, while the axes of the control windings were perpendicular to them. The output power of the Floyd’s device was partly looped in feedback to excite the process resulted in a significant power appeared in the output winding. Many investigators who successfully repeated the Floyd’s experiments (e.g. J. Naudin in France, whose design is shown in Fig. 20.11) noted that the best results of the magnetic substance “conditioning” were obtained when

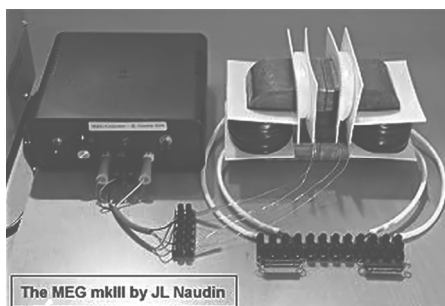


Fig. 20.11. Naudin’s Generator

discharging alternate current arc of the same frequency as the control signal directly through the permanent magnet ceramics. Thus a bistable solid-state substance was created where acoustic resonance showed at the weak control magnetic field oscillation frequency.

Special attention is attracted to the current generators based on using the “self-sustaining rotation” effect of John Serl (Mortimer, Borkshire). In the fifties of the last century he discovered that adding a small alternate current (~100 ma) radio-frequency (~10 MHz) component in the manufacturing process of permanent ceramic magnets endowed them with new and surprising properties. These consisted in the unusual interaction of the permanent magnet with the magnetic rollers located on its surface. That interaction showed in a spontaneous rolling of the rollers after applying a minor momentum to one of them.

In Russia the Serl effect was studied in the Institute of High Temperatures of Russian Academy of Science. V. Roschin and S. Godin, researches of this Institute, in 1992 built a generator similar to the Serl’s one, which they termed the “magneto-dynamic converter”. It constituted a stator with sector permanent magnets 1 and an annular rotor with rotating magnetic rollers 2 (Fig.20.12).

The rotor had a diameter of 1 m and a weight of 500 kg. The rotor segments were made on the basis of rare-earth magnets with a residual

Special attention is attracted to the current generators based on



induction of 0.85 T. They magnetized by the bank of capacitors discharging through an inductor. Unlike the Serl's disc, the ac biasing was not used in the Roschin–Godin's device. The “engagement” of the rollers with the rotor annular magnet was provided to the gear principle through transversal magnetic inserts made of NdFeB with a residual induction of 1.2 T and arranged

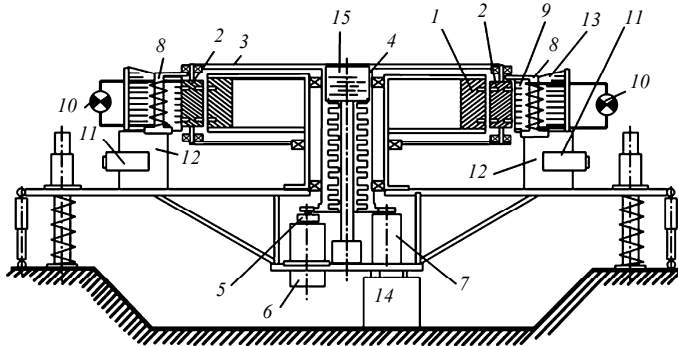


Fig. 20.12. Roschin–Godin's Converter

in the stator and the rollers. There was an air gap of 1 mm provided for in-between the stator surface and the rollers. The elements of the magnetic system were assembled as a unit construction on a platform made of non-magnetic alloys. The platform was equipped with springs, dampers and was free to move vertically along three guides, which was measured by an inductance transmitter 14. The stator 1 was fixed, while the rollers 2 secured on a mutual movable separator 3 with the help of air dynamic bearings. The separator was rigidly coupled to the shaft 4 and, through friction overrunning clutches 5, to the starting motor 6 and electrodynamic generator 7. There were electromagnetic transducers 8 with open magnetic conductors 9 positioned along the rotor. The load 10 was arranged as electric incandescent lamps. The machine was put into operation by speeding the rotor up from an electric motor. At ~550 rpm the speed of rotor rotation became spontaneously increasing despite the motor stopped with the electro-dynamic generator coupled to the shaft. To keep the speed, a load in the form of tubular electric heating elements was stepwise connected to the generator. The power output of the machine was 7 kW.

There were a number of unusual effects observed in the machine besides the “surplus power” generation, viz. platform weight reduction (to 35% of the initial weight); corona discharge in the form of a blue-pink glowing; vertical concentric zones of increased magnetic intensity (to order of 0.05 T) and abnormal temperature fall (by 6<sup>0</sup>C–8<sup>0</sup>C) in close prox-

imity to the converter. The impossibility of the existing theory to explain all these effect in whole evidences its deep inferiority.

An interesting version of a switching-reluctance device generally

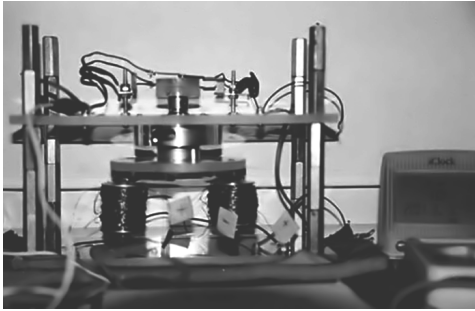


Fig. 20.13. Adams' Motor

recognized as one of the most successful “free-energy” engines was offered by Robert Adams (New Zealand) in 1977. In the Adams' motor-generator (Fig. 20.13) a rotor having permanent magnets with like poles oriented radially outside rotates generating inductive currents in the stator coils positioned around the rotor in the plane of rotation

tion. From the traditional electrical engineering standpoint a motor-generator without the closed core (coil cores have the bar configuration) is inefficient. However, this is the open core that makes it possible to generate power without rotor braking. There is no the electromagnetic induction phenomenon here in the true sense of the word, but only the magnetic induction, i.e. the magnetization and demagnetization of the stator core in the rotor permanent magnet field. It may be seen a full analogy with the electric induction, i.e. the “electrization by induction” as they would say before. The “electrization by induction” differs from the electromagnetic induction since the secondary magnetic field generated in the generator winding does not decelerate the rotor and does not interact with the primary magnetic field. Robert Adams is working together with H Aspden on acquisition of patent for his system. It is significant that operability of this machine can be completely explained as based on the Faraday's law.

The K. Minato's wheel (Patent USA No5594289, 1997) is another rotating magnets-based engine even more attractive for reproduction. It consists of a rotor (a bicycle wheel rotating on a horizontal axis) having a multiplicity of permanent magnets attached and with their like poles oriented in the rotor rotation direction, as well as stabilizers intended to balance the rotor (Fig. 20.14). Each of the permanent magnets

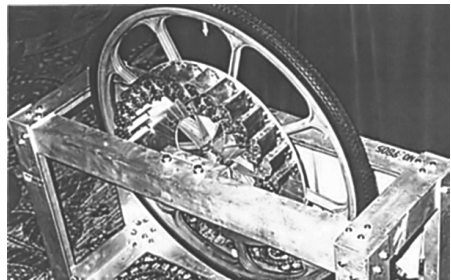


Fig. 20.14. Minato's Wheel

attached to the rotor is positioned at an angle to the wheel radius. An electromagnet with electric current periodically induced depending on the rotor rotation is arranged nearby the external periphery of the rotor closely to it. Eric Vogels (Sweden, 1997) repeated and improved the Minato's results having split the track of the magnets into a multiplicity of minor tracks.

Many patents on magnetic engines have been granted in Russia (V. Alekseenko, №5037775, 1996; V. Rykov, №2000101256, 2001; A. Rjumin, №2001123502, 2003; V. Levkin, №5032711, 1995; M. Ostrikov et al, №95103846, 1996; A. Starostin et al, №95112010, 1997; A. Kalinin, №94019782, 1996; P. Imrish, №94026259, 1996; V. Dudyshev, №2128872, 1998; Y. Pilipkov, №2000119415, 2002, etc).

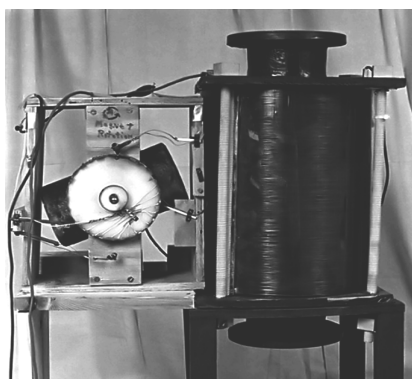


Fig. 20.15. Newman's Engine

American television network recently released the information about a revolutionary technique developed by J. Newman. His electromagnetic motor (Fig. 20.15) is capable to power a production area, residential building or farm. It is based on the concept that the motion of electrons in coil wires resembles the motion of micro-gyroscopes as electrons rotate. For high-inductance coils this motion engenders special effects showing in the "surplus power" generation. It is significant

that more that 30 physicists, nuclear engineers, electrical engineers and electricity experts signed the letter that confirmed the revolutionary character of that invention.

The homopolar induction effect known yet from Faraday's time is also capable to create electromotive force at the rotation of a metallic rotor. De Palma's homopolar generator (1991) is one of the practical designs the alternators of this class feature. The testing results on this generator (Fig. 20.16) show that its rotor deceleration due to the back EMF appears to a less degree than in the traditional generators. Therefore, system power output surpasses that required for the

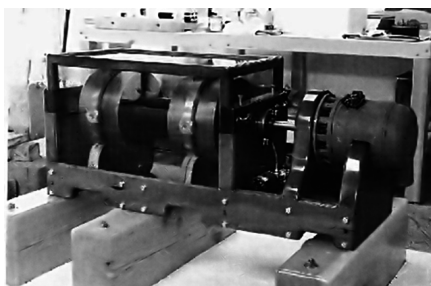


Fig. 20.16. De Palma's Generator

rotor rotation.

It is worth noticing that the creation of the alternators has already gone into a practical development stage. Swiss company SEG has quite recently announced its intention to bring to the market a generator operating on the Serl effect. It is planned to launch in the first place a compact 15-kW generator with approximate size parameters of  $46 \times 61 \times 12$  cm, which can be tuned to generate direct or alternate current of various voltage within a range of 12V to 240V. Each of such generators is capable to produce 60MW/h of energy before the reversal of the polarity would become necessary. The generator model D15AP offered is illustrated in Fig.

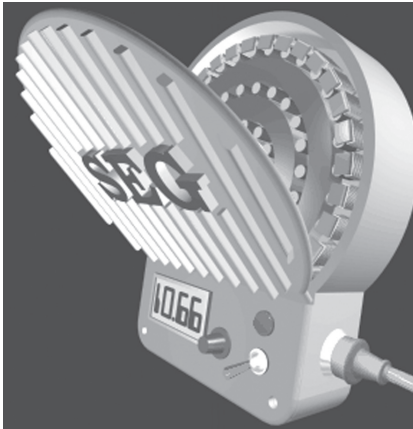


Fig. 20.17. Serl's Generator

20.17.

It consists of three four-layer concentric rings, each of the rings being made of composite. The rings are concentric to each other and attached to a base. Rollers freely rotate around each of the rings: 10 pieces around the first ring, 25 – around the second ring and 35 – around the third one. There are coils arranged outside the rollers at the external ring periphery. The coils are connected in different manner, which enables generating either direct or alternate current of various voltage. The output coils have to be calculated to provide an

output voltage of 240V at a power output of 15kW. The generator is a set of frictionless bearings in a way and, at the same time, a system of three

rotary transformers in one casing with a current of an extremely high voltage at the output.

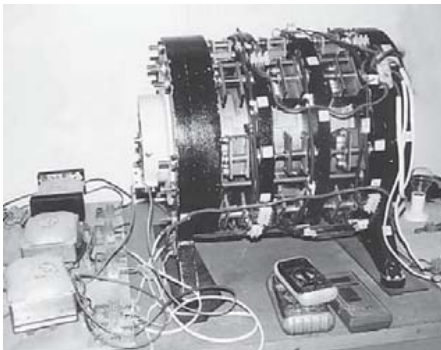


Fig. 20.18. LUTEC Generator

The LUTEC generator of Australians Brits and Christie (International Patent No00/28656, 2000) has been one of the recent additions to devices of this class. The simplicity of this engine is provided by arranging switchable coils on the stator, while a permanent

magnet – on the rotor. The direct current input to the stator coils causes

the magnetic repulsion force and is the only current to create the “aggregate motion” (Fig. 20.18).

A number of private enterprises are currently taking orders for commercial motor-generators on permanent magnets. In particular, the GMC Holding Corporation (Orlando, Florida, USA) claims that as a result of the 12-year study it has created a device on permanent magnets capable to solve the world economic problems in power engineering. Another company, Perendev (abbreviation of “perpetuum energy device”) claims that a 30kW-magnetic motor of its production is ready to find market acceptance (Fig. 20.19).

Cost estimate of the first devices is about 8,500 €. Truth to tell, Keith

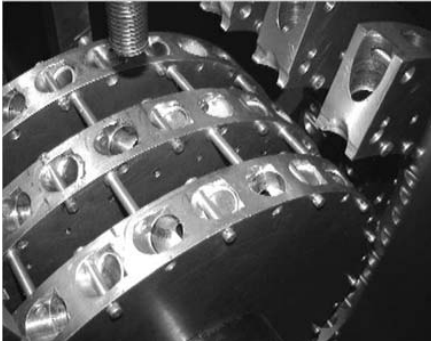


Fig. 20.19. Perendev Magnetic Motor

Anderson, whose company was invited to test the Perendev motor and built two operating analogs, claims all of them depleted their load magnets. Hence, further investigations are necessary to clarify the balance conditions for the internal energy the magnets release and their replenishment from the ambience. The key problem of the designs on permanent magnets is to calculate the magnetic flux distribution in the magnetic circuit

that may include permanent magnets, air gaps, high magnetic permeability elements and electrical currents. Accurate solutions on magnetic fields demand a complicated analysis of many factors, though approximate solutions are also acceptable based on certain

simplifying assumptions. To obtain magnets, an experience and trade-offs are often needed. Meantime, the Perendev company takes orders from those who have the adventurous spirit alive and appreciate risks and restraints of this early stage.

One more magnetic engine modification called as Cycclone<sup>1)</sup> has been recently created on funds of an American company in Australia (Fig. 20-19). A demonstrational prototype of this engine intended for a car application was shown on TV.

It is quite evident that when estimating the availability of such devices it is impermissible to consider the magnetic energy as “gratis” – its prime cost needs the same expense accounting as for any other power units on renewable power sources. These expenses depend on the magnet classes. The samarium-cobalt (SmCo) and neodymium (NdFeB) magnets

---

<sup>1)</sup> The name reflects the engine combines cyclic motion with magnetic field “cloning”.

sintered from rare-earth elements are the newest addition to the earlier known ferrite (ceramic) and aluminum-nickel-cobalt (Alnico type) magnetic materials. They feature the magnetic energy level achieved as 45–50 MGOe (mega gauss oersted). The recent developments in the magnet fabrication technique contributed to this achievement. These developments have opened new thrilling vistas toward technology upgrade of the permanent magnet engines. Besides their production costs it is reasonable to estimate also the efficient design effort and theoretical in-depth studies since the impossibility to explain the multiple effects revealing themselves in application to the alternators in operation evidences that theory is far behind experiments.

Thus we can expect the market will see small-scale power units capable to efficiently power offices, residential buildings and farms located far away from power transmission lines.

In conclusion it is desirable to underline that despite the fact the operation of alternators is obscure in many respects there are enough grounds at present to search for the most successful technical solutions on creation of new-generation converters using the practically inexhaustible energy of the ambient space.



Fig. 20.20. Cyclone Engine

## 20.5. Converters of Radiation Field energy

A dozen phenomena are known to date where after the “activation” of some working medium the heat generation during its relaxation exceeds the energy input. Such a “production” of heat energy may be observed in the oxygen–hydrogen electrolytic tanks on usual and heavy water (V. Filimonenko, 1957; S. Johns, 1989), in the electrical arresters (A. Chernetsky, 1971); vortex heat generators (Y. Potapov, 1992); at plasma and plasma-chemical dialysis (A. Frolov, 1998; F. Kanarev, 2001); at “sonoluminescence” (R. Taleyar Khan, 2002), etc. Although such phenomena were discovered a long time ago (F. Latchinov, 1888), these became known to most people after Stanly Pons and Martin Fleishman, researchers of the Utah University, had reported the results of their experiment they construed as the “cold thermonuclear fusion”. Pons and

Fleishman claimed they had observed a heating of the electrochemical element that used heavy water as an electrolyte. In that case the heat released much exceeded the electric power consumed. Fleishman assumed that the energy was generated inside the palladium cathodes in the course of the nuclear reaction where two deuterons combined into  ${}^4\text{He}$  in some manner yet unknown. However, no products of that reaction were discovered which would correspond to the heat generation as claimed. The scientific community did not recognize that claim for a scientifically substantiated explanation for several reasons. Firstly, the Coulomb barrier impedes the combination of deuterons at room temperature. The mechanism when deuterons could approach each other so that the synthesis would occur was unknown. Secondly, if they could approach each other for a reaction to occur, usual synthesis products should have been observed as they appear very soon. Thirdly, a reaction when two deuterons combine and form  ${}^4\text{He}$  usually runs with releasing gamma rays of order of 24 MeV. However, such a flow of gamma-ray emission was not observed during the experiment. Finally, the reaction in whole ran a million times faster than at usual conditions. Therefore, after many of the laboratories that attempted to reproduce that experiment had failed the scientific community came to a conclusion that the data of those experiments was incorrect. Meantime, yet in 1989 S. Johns made another statement that during electrochemical reactions in heavy water he had observed the deuteron synthesis reaction. The scientific community's response to that statement was skeptical as well since the signal/noise ratio was minor, while the theoretical considerations did not allow treating as significant the effect Johns overstressed.

Therefore, it was an unexpected sensation when in 2002 the extremely prestigious scientific magazine "Science" published an article about a desk-top thermonuclear unit R. Taley-Khan's team (USA) had created. There a small cylinder containing acetone with the hydrogen nuclei replaced by the deuterium ones was irradiated with a powerful flow of acoustic waves simultaneously with a neutron flux. The operation of the unit was claimed to have been based on the sonocavitation effect when the acoustic waves shook the water thoroughly having a multiplicity of bubbles produced there with a diameter of to 1 mm (much greater than usually), which then "collapsed". Something like this has been known since yet the thirties when it was discovered that some substances started to glow when ultrasound was passed through them (a phenomenon known as the "sonoluminescence"). Physicists affirmed that in that case acetone was heated to such temperatures that the deuterium nuclei started to merge. As in the case with the "cold thermonuclear fusion", the investigators immediately encountered troubles. The magazine "Science" that can not hazard its reputation when publishing the like sensations without

credibility check gave the floor to also other investigators who attempted to reproduce the experiment. They also discovered the neutrons. However, when they started to measure the neutron flux with a detector more advanced than in the initial test, the particles immediately disappeared. Besides, nothing proved those neutrons had something to do with the thermonuclear reaction. As a result, a good part of scientists came to a conclusion the process of such a kind just did not exist in nature.

Nevertheless, a number of investigators continue to insist on the fact that the water itself is the source of energy in such phenomena. They often refer herein to an installation known as the “Patterson cell” (USA). This installation is an electrolytic element filled with fine plastic beads covered with superfine layers of nickel. The latter, like palladium, is capable to collect and hold the heavy isotopes of hydrogen. When current is passing through the layers, electric charges appear on them. Such a device, according its producer – Patterson Power Cell (USA), steadily outputs 5W of heat power per each 1.5W input. In Patterson’s opinion the “surplus” heat in his device appears due to the cold nuclear fusion. The Patterson’s electrolytic thermal cells are currently produced by the ENECO Corporation that has collected above thirty patents with key technological solutions into a unitary patent package. The Nova Resources Group Inc. (Canada) has also launched the cells into production.

However, the physical proofs the advocates of the “cold nuclear synthesis” theory and of water as the “energy of future” source adduce are so dubious that many investigators are inclined to call it after R. Park the “voodoo science”. To make sure that some effects of the “cold nuclear synthesis” are not the reason, but rather consequence of an external impact on a system, it is enough to consider the operation of the machines wherein the “surplus heat generation” is observed at the conditions when the nuclear synthesis is excluded.

The quite sensational results Stanly Myer obtained confirming the resonance effect of electrostatic field on water molecules are among most known. In the late eighties he developed and fabricated a “low-current” water fuel electric cell (Fig. 20.21) that makes it possible to separate the usual tap water into hydrogen and oxygen with much less energy consumption than at the usual electrolysis. As S. Myer’s investigations showed, when water is exposed to a frequency coinciding with its natural molecular frequency, the chemical affinity of the hydrogen and oxygen obtained (generated as heat in the process of their subsequent synthesis) appears to exceed the energy consumed from the current source.



The design of the Myer's cell is simple. Its electrodes are made of

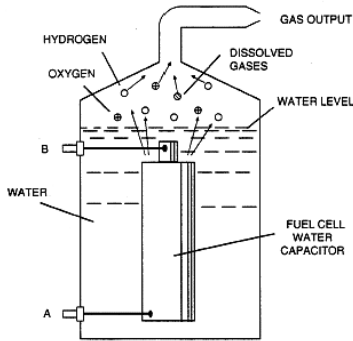


Fig. 20.21. Myer's Cell

stainless steel plates either parallel or concentric. The gas output is usually proportional to the distance between them – a good result is assured with a patented distance of 1.5 mm. Considerable distinctions from the usual electrolytic cells lie in the power supply to the cell. Myer uses an external inductance that forms an oscillation circuit with a cell capacitor to create a parallel single-tuned network. It is actuated by a powerful pulse oscillator that along with the cell capacitor

and a rectifier diode constitutes a pumping circuit. The high frequency of the pulses generates an in-step rising potential until the point reached where the water molecule disintegrates and a short current pulse appears. The meter-current supply circuit reveals this step and locks the impulse source for several cycles allowing the water recovery. Whereas the usual water electrolysis requires a current measured in amperes, the Myer's cell provides the same effect at millamperes. Furthermore, usual tap water requires an electrolyte (e.g. sulfuric acid) to be added to increase conductivity, whereas the Myer's cell operates with pure water providing a tremendous throughput. According to eye-witnesses the most striking aspect of the Myer's cell was that it remained cold even after several hours of the gas production. The recorded gas output was enough to show the oxyhydrogen flame that instantly melted the steel. To say nothing of the abundant release of oxygen and hydrogen and minimal heating of the cell, it was surprising that the water even inside the cell disappeared quickly having transformed into its components in the form of a mist spray as a great number of tiny bubbles that covered the cell surface. Myer claimed his oxyhydrogen mix converter was working for last four years based on a chain of six cylindrical cells. The Myer's invention is covered by a series of USA patents (Patents 4.936.961, 4.826.581, 4.798.661) filed before 1991 under heading "101" (where granting a patent for invention is subject to its successful demonstration). The inventor explains the cell operation by the polarization of water molecules under the electrical field gradient and the resonance within the molecule, which enhances the effect. This standpoint is close to thermokinetics which considers the low-current electrolysis as a remarkable example of the work

done by high-frequency electromagnetic oscillations applying the resonance effect to the electrons relatively weak-retained.

Some investigators explain the surplus heat appearing by the water molecular structure reconfiguration. Actually, tens of the water molecular structure modifications are known which evidently differ in also their internal energy. In such a case the water transit from one configuration into another with a lower energy level must involve a heat release. In particular, as Dr. R. Mills (USA) sees it, the hydrogen atoms in the water molecule may be at different energy sublevels including also those corresponding to fractional quantum numbers. He called the water molecules with hydrogen atoms being at a lower (than usual) energy level as “hydrino” (see also S. Nesterov, 1995). However, this standpoint contradicts quantum physics and meets, therefore, many opponents.

Meantime, there may exist another and quite adequate to the existing paradigm explanation of the surplus heat release phenomenon in the above processes. For this it is necessary to recognize the fact that the “heat generators” above described operate as heat pumps. They feature the reverse cycle “water electrolysis – hydrogen and oxygen synthesis” where the dissipated radiant environmental energy is a heat well analog, while the work spent for electrolysis – an analog of compression work in heat engines.

Released heat  $Q$  to power supply energy  $W$  ratio called as heat transformation coefficient  $\eta_r$  in thermodynamics is known to be the efficiency criterion for inverse cycles:

$$\eta_r = Q/W > 1, \quad (20.5.1)$$

This criterion always exceeds unity if only  $W$  is construed as the work a source of current supply spends. However, this not at all means the “over-unity” efficiency  $\eta_i = W/Q$  obtained since the efficiency is construed as a reciprocal, viz. work  $W$  obtained in engine related to heat  $Q$  supplied from “hot” well.

The experiments conducted by Wm. Lyne (1996) are further evidence that the field (distinguished from substance) forms of energy of the ambient space are a source of surplus heat energy at the spontaneous synthesis of hydrogen and oxygen molecules in the Myer’s installation. In 1981 Lyne built and tested a heating system on atomic hydrogen. The hydrogen in his installation, like at the usual hydrogen welding, passed through electric arc which decomposed it into “atomic” hydrogen. Then the atomic hydrogen recombined under heat release. Thus the hydrogen played a part of a “mediator” that ran through a cyclic process, while the electric power consumption to maintain the arc was considered by Lyne

as an “activation” energy. The energy “lacking” for the hydrogen dissociation was taken, in Lyne’s opinion, from the “ether”.

Similar results are obtained in tests with heat generators on atomic hydrogen, which have been conducted in Russia since 2003 by A. Frolov, founder of the Faraday Lab. Ltd (JSC LNTF). His design is based on a powerful electron-vacuum diode with the tungsten directly heated cathode (Fig. 20.22).

The generator includes a cylinder with inlet and outlet channels where the water stream flows around a closed internal chamber filled with hydrogen at a pressure of 0.2 at. The diode tungsten filament with a diameter of 0.25 mm in the center of the device serves as a cathode whereon the hydrogen changes from molecular state into atomic one. Then during the H-to-H<sub>2</sub> transit a “surplus” heat is released, which is removed with the cooling water. Hydrogen is not consumed here. To create the “low-current” splitting of H<sub>2</sub> into H, a potential difference with pulses within 200 V to 300 V is applied between positive anode and negative cathode. The pulses are generated by direct current with a frequency of to 10 MHz. When using the cathode pulse heating of 12 V with a frequency of 51 Hz and a pulse/break ratio of 5%, a multiple excess of the heat produced over the electrical power consumed is obtained. It is significant that the anode voltage pulses generated by alternate current do not cause this effect. These experiments obviously enough confirm the above “thermokinetic” interpretation of the “surplus” heat production origin. The absence of the hydrogen consumption evidences that hydrogen is here just a “mediator” (working medium), but not the energy source, while the absence of the “surplus heat generation” effect with ac supply to anode confirms the fact that this effect is obtained not by the “excitation” of orbital electrons at their mean energy level invariable, but rather by the unilateral action of the voltage pulses in the direction of removing the orbital electrons from the hydrogen nucleus (in resonance with pulses of the electromagnetic field surrounding the device). The selection of the anode voltage pulse frequency is necessary in this case in order to obtain resonance between the external field action and the “activation” pulses.

French investigator J. L. Naudin has recently improved the operation of this generator replacing the power unit by a large-capacity battery with

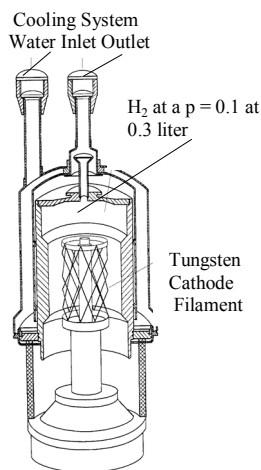


Fig. 20.22. Frolov’s Generator

a 10 MHz-pulse generator. On this basis Naudin managed to better form the anode voltage pulse, which configuration appeared have been very important, and thus to build up the “heat output”. His “atomic hydrogen generator” was in operation for an hour with an efficiency exceeding 2,000%, i.e. with 20-fold exceed of the heat generation over the electrical power consumed. He used two types of absolutely different measuring instrumentation which confirmed the reliability of input power measurement for the installation.

Y. Potapov’s “heat generator” (Patent of RF №2045715, 1993) is one of the widely known devices intended for practical using “surplus” heat

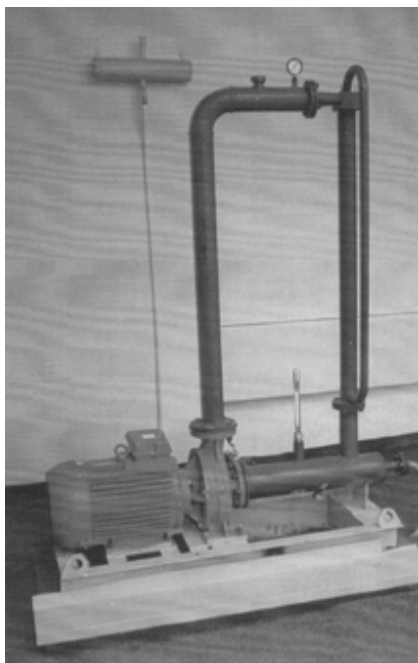


Fig. 17.23. Y. Potapov’s Heat Generator

generation. It constitutes a vertical cylindrical tube with a water flow tangential input in its upper part (Fig. 17.23). The velocity of the water is such that there are cavitation phenomena causing quick water heating and observed in the tube along with the intensive flow turbulence. If this water is removed from the maximal temperature zone and directed to usual heating devices with return to the lower part of the vortex tube (wherefrom it is taken by a usual centrifugal pump and pumped again to the upper part of the tube), the amount of the heat removed for heating appears to exceed the amount as to the balance of the dissipative (hydrodynamic) losses for friction and cavitation. From the author’s initial statements his heat generator produced up to 3 to

4 kW of heat per 1 kW of the electrical power consumed. However, at comparative testing in NPO «Energia» in 1996 the heat generation in the Potapov’s device appeared to have been only 23% higher than in the 3-phase ac electrode boiler and 42% higher than in the electrical boilers with standard heating elements (tubular electric heating elements). In Potapov’s opinion the surplus heat generation in his installation is explained basically by the integration of water molecules in “associates” under the cavitation effect and, to a lesser degree, by the cold nuclear fusion reactions (Y. Potapov et al, 2002). This standpoint is supposedly supported by the discovered in the HPO «Energia» 1.5-increase in the hard gamma ra-

diation (not mitigated with steel shield) and the generation of carbon radioactive isotopes if the installation filled in with an anti-freezing agent.

At the same time the author has repeatedly stressed that the water in the installation may not be interchanged for several years. This means that the water and the anti-freezing agent were actually just a working medium participating in the closed process, whereas a primary energy source should be searched for beyond it. This is the opinion F. Kanarev (2004). He thinks physical vacuum to be the “surplus” heat generation source.

The surplus heat generation phenomenon theoretically allows creating autonomous (self-sustained) power supply sources. To create them, it is necessary to combine electrolysis cell with fuel cell or heat engine converting heat  $Q$  obtained at burning of oxyhydrogen mixture into electric power  $W$ . According to thermodynamics the efficiency of such a machine will be dependent on the temperature  $T$  of the heat  $Q$  yielding from synthesis or recombination. If the temperature of the heat obtained as a result of synthesis or recombination exceeds that of the ambient space  $T_0 \approx 300$  K by just 30K, ideally the Carnot engine built on this heat source will have the thermal efficiency only 9%. This means that, to cover the energy expended on electrolysis, a more that 11-fold “surplus heat” output is needed.

Nevertheless, the thermokinetic analysis undertaken herein is meant to mitigate the suspicion of formal science toward the phenomena above described and to switch the problem of creating electrical energy alternative sources to practical course. Several firms are already selling cavitation heating equipment. Formal science is looking askance at this trade activity, the more so because the surplus heat generation in this equipment is not supported with independent expert appraisal data. However, profit of trade appears to be dominating. As reported at the Genesis World energy consortium’s site, they have already developed a self-contained and self-sustained energy generator “Edison Device”. In its size it is approximates to the external air conditioning system, which makes it possible to quickly and easily install it at home or in office to obtain a practically unlimited energy from any available water source. The commercial model of the device is capable to generate 100 kW of energy per diem. The “mechanical part” comprises minor pumps and micro-valves providing a circulation, which makes the device noiseless and not demanding a special maintenance for the designed 20-year service life. The feasibility of such environmental energy converters are also confirmed by the valid tests on the Mayer’s converters in motor car application. Water consumption per a haul of 100 km was there about 3 liters (Pat. USA No 149.407). Thus the point is just to find the most promising engineering solutions in this field.

## Conclusions to Part 5

Applying energodynamics to systems doing useful work has made it possible to set and solve a number of new interesting problems. Laying foundations of similarity theory for linear power converting systems should first of all be noted among them. This theory has first confirmed in most general the unity of general regularities of energy conversion in heat and non-heat, cyclic and non-cyclic, direct and inverse machines. It has thereby uprooted the inconsistency of attempts to restrict the application of classic thermodynamic laws to only heat engines. Practical importance of this theory is that it allows transferring the investigation results from one (well studied) power and process installations to another (little studied). The examples given in this chapter confirm this.

Laying foundations of productivity theory for technical systems has become not less important achievement of energodynamics. Enabling the synthesis of thermokinetics and thermoeconomics this theory supplements the classic analysis of thermodynamic efficiency for power units by correlating their power and economic efficiency. Thereby it approximates the thermodynamic estimates of limiting potentials for irreversible processes to reality. At the same time this theory allows finding the economically most advantageous operational modes for various power, process and transport units, which is of great practical importance. The theory application examples given in this chapter demonstrate that the conclusions from thermokinetic are of the same strictness and generality degree as those from thermodynamics with regard to reversible processes.

However, most “exotic” are perhaps the deductions of energodynamics about the possibility of using field forms of energy. These results allow explaining the functionality of a number of devices presently referred to “perpetuum mobile”. The energodynamic analysis given in this chapter and pertaining to devices consuming the energy of gravitational, electrostatic and electromagnetic fields demonstrates that the operation of these devices does not exceed the bounds of energodynamics and does not conflict with its laws. Lifting theoretical bans on creation of such devices opens new vistas to using renewable energy sources alternative to the known ones and actually inexhaustible.